IEEE Access
Multidisciplinary | Rapid Review | Open Access Journal

Received July 14, 2020, accepted July 31, 2020, date of publication August 4, 2020, date of current version August 28, 2020.

Digital Object Identifier 10.1109/ACCESS.2020.3014220

Minimum-Learning-Parameter-Based Fault-Tolerant Control for Spacecraft Rendezvous With Unknown Inertial Parameters

YUAN LIU[1], HUI ZHANG[2], SAI ZHANG[3], HANG LI[2], CHENGYI LI[2], JING REN[2], MENGYU QIU[2], AND QI WU[4]

[1]School of Astronautics, National University of Defense Technology, Changsha 410022, China
[2]China Academy of Space Technology, Beijing 100094, China
[3]College of Aerospace and Civil Engineering, Harbin Engineering University, Harbin 150001, China
[4]China Aero Engine Control System Research Institute, Wuxi 214063, China

Corresponding author: Yuan Liu (stephenliuyuan@souhu.com)

This work was supported in part by the National Key Research and Development Program of China under Grant 2016YFB0501003, and in part by the Major Program of National Natural Science Foundation of China under Grant 61690214.

ABSTRACT In this paper, robust control strategies are explored to solve the problem of rendezvous maneuver for rigid spacecraft exposed to the external disturbance, actuator faults and unknown inertial parameters. To pursue the control objective, two adaptive controllers are constructed via the sliding mode control (SMC) technology. Firstly, a basic control scheme is designed in the event of unknown inertial parameters and external disturbance, where the Minimum-learning-parameter (MLP) algorithm is adopted for approximating the unknown system dynamics. Though effective, the basic controller is not applicable in the actuator fault scenarios. Considering this drawback, adaptive laws are designed in the second controller to tackling the actuator faults. It is illustrated that the proposed controllers will endow tracking errors with asymptotic stability and strong robustness to actuator faults. Finally, the effectiveness of the control strategies is verified by numerical simulations.

INDEX TERMS Spacecraft rendezvous maneuver, fault-tolerant control, unknown inertial parameters, minimum-learning-parameter.

I. INTRODUCTION

Recently, spacecraft rendezvous technology has elicited widespread interest due to its distinctly important role in variety of space missions, such as Mars exploration, space object capturing, deep space exploration, etc. To successfully complete these missions, rendezvous maneuver control system must be designed with satisfactory performance. However, it is still a challenging work to construct such kind of controllers owing to the complexity of the external disturbance, unknown system dynamics and unexpected actuator faults. Despite of these difficulties, researchers have developed numerous strategies for spacecraft tracking control, including adaptive control [1]–[5], backstepping control [11]–[13], output feedback control [25], [26] and sliding mode control [4], [18], [19], [31]–[33].

In various space activities, the inertial parameters may remain unknown to designers, which is mainly caused by the fuel consumptions and onboard payload variations. However, the inertial parameters are assumed to be exactly available in the foregoing results. To overcome this drawback, fruitful results has been reported recently [1]–[8]. In [1], an adaptive SMC method has been proposed for the liquid-filled spacecraft in the presence of unknown inertia and external disturbances. Taking the convergence rate into account, an inertial parameter identification algorithm has been exploited with globally finite-time stability being ensured [2]. Obviously, controllers in [1], [2] are only applicable for single spacecraft control issues. For the multiple spacecraft coordinated control problem, adaptive laws were designed for

The associate editor coordinating the review of this manuscript and approving it for publication was Ning Sun.

estimating unknown parameters in [3], where a dynamic adjustment function was established to optimize the control gains. As a technological extension of [3], the passive fault-tolerant control strategy was applied to handle the actuator failures for spacecraft formation flying [4]. It is noteworthy that results in [1]–[6] cannot be directly utilized for rendezvous maneuver. Considering unknown inertial parameters in rendezvous cases, a linear operator-based control architecture was designed via backstepping design [7]. Different from the method in [7], the external disturbance is estimated online through disturbance observer [8].

It must be noted that the unknown inertia parameters were handled via adaptive laws in [7], [8]. As an alternative for this issue, neural network and fuzzy logic possess desirable abilities in approximating uncertain nonlinear dynamics caused by unknown parameters, leading to numerical applications in aerospace engineering [9]–[15]. In [9], the convolutional neural network has been applied to obtain the pose estimation for spacecraft during rendezvous process. Considering the adverse influence caused by the J2 perturbations, an adaptive neural network controller was exploited for spacecraft rendezvous, where the nonlinear dynamical models were established [10]. In [11], the backstepping based neural network control method was applied to deal with the uncertainties for spacecraft rendezvous. Besides the neural networks, the fuzzy logics can also identify the unknown system dynamics with satisfactory performance [12]–[15]. When the neural networks were utilized for spacecraft rendezvous in [9]–[11], the weight matrix must be updated online, thus causing much computational complexity. Consequently, it is imperative to design controllers for spacecraft rendezvous with less computational complexity.

Besides the unknown inertia parameters and external disturbances, the actuator fault is another aspect in spacecraft rendezvous deserving special attention. Owing to the complexity of the space environment, actuator failures always occur during rendezvous maneuver, which heavily threaten the safety of the spacecraft. To improve the reliability of the control system, fault-tolerant control strategies have been widely developed for spacecraft rendezvous [16], [17], [21]–[25]. In [16], with the utilization of a modified integral sliding mode control strategy, the actuator failure could be properly compensated for limited-thrust spacecraft rendezvous. The controller in [16] was designed on the basis of passive fault-tolerant control strategy, while an active controller was presented in [17], where the information of the fault was identified online. Though effective, controllers in [16] and [17] can only ensure asymptotic stability for the closed-loop system. To derive controllers with faster convergence rate for rendezvous maneuver, fixed-time controllers were designed in [18]–[20]. When the actuator and the unknown inertia parameters were considered simultaneously, an effective controller was designed in [21], where the bondedness of signals could be ensured. Reviewing the existing results for spacecraft rendezvous, it can be found that the actuator failures, unknown inertia parameters and computational complexity are rarely treated simultaneously.

Inspired by the above observations, this paper will investigate the robust control for spacecraft rendezvous with actuator faults and unknown inertia parameters. The contribution of this paper can be summarized as follows:

i) Compared with the existing literatures utilizing the neural networks [9]–[11], the MLP algorithm is adopted in the controller design process, which will reduce the computational complexity to some extent.

ii) The chattering problem can be solved by the algorithm proposed in this paper. Here, the hyperbolic tangent function will be applied in the control law, where the adverse effect caused by chattering can be avoided.

The rest of this paper is arranged as follows. The dynamics model of the spacecraft and preliminaries are given in section 2. The controller is developed in section 3. Simulation results can be found in section 4. Section 5 concludes this work.

II. SPACECRAFT MODEL AND PRELIMINARIES

A. RELATIVE ATTITUDE DYNAMIC MODEL

The control equations for the attitude motion of a rigid spacecraft can be established by using the unit quaternion. According to [22], the rotation matrix $\boldsymbol{R} \in SO(3)$ and the unit quaternion $\boldsymbol{Q} = \left[q_0, \boldsymbol{q}_v^{\mathrm{T}}\right]^{\mathrm{T}} \in \Xi$ with $\Xi = \left\{\boldsymbol{Q} \in \mathbb{R} \times \mathbb{R}^{3\times 3} \,|q_0^2 + \boldsymbol{q}_v^{\mathrm{T}}\boldsymbol{q}_v = 1\right\}$ are applied in attitude formulation. Furthermore, $\boldsymbol{Q}_p$ and $\boldsymbol{Q}_t$ represent the attitude of the pursuer and the target, respectively. Consequently, the relative attitude between the pursuer and the target can be expressed as follows:

$$\tilde{\boldsymbol{Q}} = \left[\tilde{q}_0, \tilde{\boldsymbol{q}}_v\right]^{\mathrm{T}} = \boldsymbol{Q}_p^{-1} \odot \boldsymbol{Q}_t \tag{1}$$

According to the theory in [28], the relative attitude kinematics can be given as:

$$\dot{\tilde{q}}_0 = -\frac{1}{2}\tilde{\boldsymbol{q}}_v^{\mathrm{T}}\tilde{\boldsymbol{\omega}} \tag{2}$$

$$\dot{\tilde{\boldsymbol{q}}}_v = \frac{1}{2}\left(\tilde{\boldsymbol{q}}_v^{\times} + \tilde{q}_0\boldsymbol{I}_3\right)\tilde{\boldsymbol{\omega}} \tag{3}$$

where $\boldsymbol{\omega}_p$ is the angular velocity of the pursuer; $\boldsymbol{\omega}_t$ is the angular velocity of the target. Consequently, the relative angular velocity $\tilde{\boldsymbol{\omega}}$ can be defined as $\tilde{\boldsymbol{\omega}} = \boldsymbol{\omega}_p - \tilde{\boldsymbol{R}}\boldsymbol{\omega}_t$. For any vector $\boldsymbol{a} = [a_1, a_2, a_3]^{\mathrm{T}}$, it defines $\boldsymbol{a}^{\times}$ as Eq. (4). The rotation matrix is defined as Eq. (5).

$$\boldsymbol{a}^{\times} = \begin{bmatrix} 0 & -a_3 & a_2 \\ a_3 & 0 & -a_1 \\ -a_2 & a_1 & 0 \end{bmatrix} \tag{4}$$

$$\tilde{\boldsymbol{R}} \triangleq \boldsymbol{R}\left(\tilde{\boldsymbol{q}}\right) = \left(\tilde{q}_0^2 - \tilde{\boldsymbol{q}}_v^{\mathrm{T}}\tilde{\boldsymbol{q}}_v\right)\boldsymbol{I}_3 + 2\tilde{\boldsymbol{q}}_v\tilde{\boldsymbol{q}}_v^{\mathrm{T}} - 2\tilde{q}_0\tilde{\boldsymbol{q}}_v^{\times} \tag{5}$$

Then, the corresponding attitude dynamics can be given as

$$\boldsymbol{J}_t\dot{\boldsymbol{\omega}}_t + \boldsymbol{\omega}_t^{\times}\boldsymbol{J}_t\boldsymbol{\omega}_t = 0 \tag{6}$$

$$\boldsymbol{J}\dot{\boldsymbol{\omega}}_p + \boldsymbol{\omega}_p^{\times}\boldsymbol{J}\boldsymbol{\omega}_p = \boldsymbol{\tau} + \boldsymbol{\tau}_d \tag{7}$$

where $\boldsymbol{J}_t \in \mathbf{R}^{3\times3}$ and $\boldsymbol{J} \in \mathbf{R}^{3\times3}$ are the inertia matrices of the target and pursuer, respectively; $\boldsymbol{\tau} \in \mathbf{R}^3$ and $\boldsymbol{\tau}_d \in \mathbf{R}^3$ express the control torque and the external disturbance torque, respectively.

The derivative of $\tilde{\boldsymbol{\omega}}$ satisfies

$$\dot{\tilde{\boldsymbol{\omega}}} = \dot{\boldsymbol{\omega}}_p - \dot{\tilde{\boldsymbol{R}}}\boldsymbol{\omega}_t - \tilde{\boldsymbol{R}}\dot{\boldsymbol{\omega}}_t \tag{8}$$

In terms of the definition $\dot{\tilde{\boldsymbol{R}}} = \tilde{\boldsymbol{R}}\tilde{\boldsymbol{\omega}}^{\times}$ and Eqs. (6)-(8), it can conclude that

$$\boldsymbol{J}\dot{\tilde{\boldsymbol{\omega}}} = -\boldsymbol{C}_r\tilde{\boldsymbol{\omega}} - \boldsymbol{n}_r + \boldsymbol{\tau} + \boldsymbol{\tau}_d \tag{9}$$

where $\boldsymbol{C}_r = \boldsymbol{J}\left(\tilde{\boldsymbol{R}}\boldsymbol{\omega}_t\right)^{\times} + \left(\tilde{\boldsymbol{R}}\boldsymbol{\omega}_t\right)^{\times}\boldsymbol{J} - \left(\boldsymbol{J}\left(\tilde{\boldsymbol{\omega}} + \tilde{\boldsymbol{R}}\boldsymbol{\omega}_t\right)\right)^{\times}$ and $\boldsymbol{n}_r = \left(\tilde{\boldsymbol{R}}\boldsymbol{\omega}_t\right)^{\times}\boldsymbol{J}\tilde{\boldsymbol{R}}\boldsymbol{\omega}_t + \boldsymbol{J}\tilde{R}\dot{\boldsymbol{\omega}}_t$.

B. RELATIVE ORBIT DYNAMICS MODEL

The pursuer's position $\boldsymbol{r_p}$ and velocity $\boldsymbol{v_p}$ can be expressed as Eq. (10) and Eq. (11), respectively.

$$\boldsymbol{r_p} = \tilde{\boldsymbol{r}} + \tilde{\boldsymbol{R}}\left(\boldsymbol{r}_t + \boldsymbol{\sigma}_t\right) \tag{10}$$

$$\boldsymbol{v_p} = \tilde{\boldsymbol{v}} + \tilde{\boldsymbol{R}}\left(\boldsymbol{v}_t + \boldsymbol{\omega}_t^{\times}\boldsymbol{\sigma}_t\right) \tag{11}$$

Here, $\boldsymbol{r}_t$ and $\boldsymbol{v}_t$ are the target's position and velocity; $\tilde{\boldsymbol{r}}$ and $\tilde{\boldsymbol{v}}$ are the relative position and velocity, respectively; $\boldsymbol{\sigma}_t \in R^3$ is a constant vector denoting the desired rendezvous position. The derivative of Eq. (10) can be expressed as follows:

$$\dot{\boldsymbol{r}}_{\boldsymbol{p}} = \dot{\tilde{\boldsymbol{r}}} + \dot{\tilde{\boldsymbol{R}}}\left(\boldsymbol{r}_t + \boldsymbol{\sigma}_t\right) + \tilde{R}\dot{\boldsymbol{r}}_t \tag{12}$$

Then, similar to the analysis in [27], it is obtained that:

$$\dot{\boldsymbol{r}}_t = \boldsymbol{v}_t - \boldsymbol{\omega}_t^{\times}\boldsymbol{r}_t \tag{13}$$

$$\dot{\boldsymbol{r}}_{\boldsymbol{p}} = \boldsymbol{v_p} - \boldsymbol{\omega}_p^{\times}\boldsymbol{r_p} \tag{14}$$

Combining Eq. (12) and Eq. (14) yields

$$\dot{\tilde{\boldsymbol{r}}} + \dot{\tilde{\boldsymbol{R}}}\left(\boldsymbol{r}_t + \boldsymbol{\sigma}_t\right) + \tilde{\boldsymbol{R}}\dot{\boldsymbol{r}}_t = \boldsymbol{v_p} - \boldsymbol{\omega}_p^{\times}\boldsymbol{r_p} \tag{15}$$

The derivative of $\tilde{\boldsymbol{r}}$ will be given as:

$$\dot{\tilde{\boldsymbol{r}}} = \tilde{\boldsymbol{v}} - \boldsymbol{C}_t\tilde{\boldsymbol{r}} \tag{16}$$

where $\boldsymbol{C}_t = \left(\tilde{\boldsymbol{\omega}} + \tilde{\boldsymbol{R}}\boldsymbol{\omega}_t\right)^{\times}$. Consequently, the derivative of Eq. (11) can be obtained as

$$\dot{\boldsymbol{v}}_{\boldsymbol{p}} = \dot{\tilde{\boldsymbol{v}}} + \dot{\tilde{\boldsymbol{R}}}\left(\boldsymbol{v}_t + \boldsymbol{\omega}_t^{\times}\boldsymbol{\sigma}_t\right) + \tilde{\boldsymbol{R}}\left(\dot{\boldsymbol{v}}_t + \dot{\boldsymbol{\omega}}_t^{\times}\boldsymbol{\sigma}_t\right) \tag{17}$$

Position dynamics of the spacecraft can be written as Eqs. (18)-(19) through the theory in [27].

$$m_t\dot{\boldsymbol{v}}_t + m_t\boldsymbol{\omega}_t^{\times}\boldsymbol{v}_t = 0 \tag{18}$$

$$m_p\dot{\boldsymbol{v}}_p + m_p\boldsymbol{\omega}_p^{\times}\boldsymbol{v}_p = \boldsymbol{f} + \boldsymbol{f}_d \tag{19}$$

Here, m_t and m_p are constants defining masses of the target and the purser, respectively; $\boldsymbol{f} \in \mathrm{R}^N$ and $\boldsymbol{f}_d \in \mathrm{R}^3$ denote the control force and external disturbance force. Combining Eq. (17) and Eq. (19), it follows that [27]

$$m_p\left[\dot{\tilde{\boldsymbol{v}}} + \dot{\tilde{\boldsymbol{R}}}\left(\boldsymbol{v}_t + \boldsymbol{\omega}_t^{\times}\boldsymbol{\sigma}_t\right) + \tilde{\boldsymbol{R}}\left(\dot{\boldsymbol{v}}_t + \dot{\boldsymbol{\omega}}_t^{\times}\boldsymbol{\sigma}_t\right)\right] + m_p\boldsymbol{\omega}_p^{\times}\boldsymbol{v}_p = \boldsymbol{f} + \boldsymbol{f}_d \tag{20}$$

That is

$$m_p\dot{\tilde{\boldsymbol{v}}} = -m_p\boldsymbol{C}_t\tilde{\boldsymbol{v}} - m_p\boldsymbol{n}_t + \boldsymbol{f} + \boldsymbol{f}_d \tag{21}$$

where $\boldsymbol{n}_t = \left(\tilde{\boldsymbol{R}}\boldsymbol{\omega}_t\right)^{\times}\tilde{\boldsymbol{R}}\boldsymbol{v}_t + \tilde{R}\dot{\boldsymbol{v}}_t + \tilde{\boldsymbol{\omega}}^{\times}\tilde{\boldsymbol{R}}\tilde{\boldsymbol{\sigma}}_t^{\times}\boldsymbol{\omega}_t - \tilde{\boldsymbol{R}}\tilde{\boldsymbol{\sigma}}_t^{\times}\dot{\boldsymbol{\omega}}_t$.

In this paper, it assumes that the actuator fault signals are identified and satisfy:

$$\boldsymbol{\tau} = \boldsymbol{\delta}_r\boldsymbol{\varepsilon}_r, \quad \boldsymbol{f} = \boldsymbol{\delta}_t\boldsymbol{\varepsilon}_t \tag{22}$$

$\boldsymbol{\delta}_r \in \mathrm{R}^N$ and $\boldsymbol{\delta}_t \in \mathrm{R}^N$ are diagonal matrices denoting the faults coefficients. Combining Eq. (9), Eq. (21) and Eq. (22), the relative dynamics can be established as follows:

$$\mathbf{J}\dot{\tilde{\boldsymbol{\omega}}} = -\boldsymbol{C}_r\tilde{\boldsymbol{\omega}} - \boldsymbol{n}_r + \boldsymbol{\delta}_r\boldsymbol{\varepsilon}_r + \boldsymbol{d}_r \tag{23}$$

$$m\dot{\tilde{\boldsymbol{v}}} = -m\boldsymbol{C}_t\tilde{\boldsymbol{v}} - m\boldsymbol{n}_t + \boldsymbol{\delta}_t\boldsymbol{\varepsilon}_t + \boldsymbol{d}_t \tag{24}$$

where $\boldsymbol{d}_r = \boldsymbol{\tau}_d$ and $\boldsymbol{d}_t = \boldsymbol{f}_d$.

To complete the controller design for spacecraft rendezvous maneuver, the exact motion information of the target spacecraft is supposed to be available to the tracker spacecraft. Then, this paper is dedicated to designing control torques $\boldsymbol{\varepsilon}_r$ and $\boldsymbol{\varepsilon}_t$ for the dynamics expressed by Eq. (23) and Eq. (24) such that the relative valuables $\tilde{\boldsymbol{r}}$, $\tilde{\boldsymbol{v}}$, $\tilde{\boldsymbol{q}}_v$ and $\tilde{\boldsymbol{\omega}}$ can be stabilized even in the presence of actuator failures.

To proceed further, the following assumptions are given.

Assumption 1: In this paper, one can suppose that $\boldsymbol{d}_r$ and $\boldsymbol{d}_t$ are unknown external disturbances, which satisfy $\|\boldsymbol{d}_r\| \le D_r$, $\|\boldsymbol{d}_t\| \le D_t$. Here, D_r and D_t are positive constants.

Assumption 2: Classically, the target spacecraft is stable during the mission of the rendezvous maneuver. In terms of Eqs. (2), (3), (23) and (24), it infers that the equations $\|\boldsymbol{\omega}_t\| \le a_1$, $\|\dot{\boldsymbol{\omega}}_t\| \le a_2$, $\|\boldsymbol{v}_t\| \le a_3$ and $\|\dot{\tilde{\boldsymbol{v}}}_t\| \le a_4$ are satisfied, where a_1, a_2, a_3, a_4 are unknown constants.

Assumption 3: The inertia matrix $\boldsymbol{J}$ is an unknown but bounded parameter, which satisfies $\lambda_1\boldsymbol{I}_{3\times3} \le \boldsymbol{J} \le \lambda_2\boldsymbol{I}_{3\times3}$ with λ_1 and λ_2 being positive constants.

C. FUNCTION APPROXIMATION BASED ON RADIAL BASIS FUNCTION NEURAL NETWORKS (RBF NNs)

RBF NNs is an effective tool to accomplish the purpose of function approximation. Therefore, this method has been extensively used in controller design for nonlinear system with unknown dynamics. In this paper, the unknown system dynamics caused by the uncertain inertia matrix can be solved by RBF NNs. To promote the process of controller design, the following lemmas should be mentioned firstly.

Lemma 1 [29]: It must be mentioned that the ideal weight vector $\boldsymbol{W}$ can be applied to express the equivalent expression of the stochastic continuous function $f(x)$, that is

$$f(\boldsymbol{x}) = \boldsymbol{W}^{\boldsymbol{T}}\boldsymbol{h}(\boldsymbol{x}) + \varepsilon \tag{25}$$

where $\boldsymbol{W} = [W_1, W_2, \ldots, W_p]^{\mathrm{T}}$ is the weight vector and $\boldsymbol{x} = [x_1, x_2, \ldots, x_m]$ is the input vector; p and m are the node number of $\boldsymbol{W}$ and input number of v, respectively; ε is the additional approximation error; $\boldsymbol{h}(\boldsymbol{x}) = [h_1(\boldsymbol{x}), \ldots, h_m(\boldsymbol{x})]^{\mathrm{T}}$

is the Gaussian basis function vector which can be defined as:

$$h_i(\boldsymbol{x}) = \exp\left(-\frac{\|\boldsymbol{x}-\boldsymbol{c_i}\|_2^2}{2b_i^2}\right), \quad i = 1, \ldots, p \tag{26}$$

where $\boldsymbol{c_i} \in R^{\mathrm{m}}$ and $b_i \in R$ denote the center vector and the Gaussian basis function vector of $h_i(\boldsymbol{x})$, respectively.

D. PRELIMINARIES

Notations: For a vector $\boldsymbol{\xi} = [\xi_1, \xi_2, \ldots, \xi_n]^{\mathrm{T}}$, $\tanh^2(\boldsymbol{\xi}) = \left[(\tanh(\xi_1))^2, (\tanh(\xi_2))^2, \ldots, \tanh(\xi_n)\right]^{\mathrm{T}}$. The notation $\|\cdot\|$ defines the Euclidean norm of a vector or the induced norm of a matrix.

For matrix $\boldsymbol{W}^* = \left[\boldsymbol{W}_1^*, \boldsymbol{W}_2^*, \boldsymbol{W}_3^*\right]^{\mathrm{T}}, \boldsymbol{h} = [\boldsymbol{h}_1, \boldsymbol{h}_2, \boldsymbol{h}_3]^{\mathrm{T}}$, the notation $\boldsymbol{W}^* \circ \boldsymbol{h}$ can be defined as

$$\boldsymbol{W}^* \circ \boldsymbol{h} = \begin{bmatrix} \boldsymbol{W}_1^{*\mathrm{T}}\boldsymbol{h}_1 \\ \boldsymbol{W}_2^{*\mathrm{T}}\boldsymbol{h}_2 \\ \boldsymbol{W}_3^{*\mathrm{T}}\boldsymbol{h}_3 \end{bmatrix} \tag{27}$$

Lemma 2 [29]: For arbitrary real number $x \in R$, $\mu > 0$ and $\kappa = 0.2785$, the relation Eq. (28) exists.

$$0 < |x| - x\tanh(\mu x) \leq \frac{\kappa}{\mu} \tag{28}$$

III. CONTROLLER DESIGN

A. BASIC CONTROLLER DESIGN

In order to render the system Eq. (23) and Eq. (24) with asymptotic stability, a nonlinear controller based on the SMC theory is presented in this section. Firstly, it assumes that all actuators work normally and the external disturbance possesses an upper bound. Then, the basic control algorithm is applied to deal with the unknown dynamics and external disturbances. More specifically, the RBF NNs is used to estimate the unknown model information and the hyperbolic tangent function is exploited to deal with the chattering problems.

Inertially, two sliding mode variables can be constructed as:

$$\boldsymbol{s}_1 = \dot{\tilde{\boldsymbol{q}}}_{\mathrm{v}} + k_1\tilde{\boldsymbol{q}}_{\mathrm{v}} \tag{29}$$

$$\boldsymbol{s}_2 = \dot{\tilde{\boldsymbol{r}}} + k_2\tilde{\boldsymbol{r}} \tag{30}$$

where k_1 and k_2 are positive constants. In terms of Eqs. (3), (9), (16), (20), (29) and (30), the derivatives of $\boldsymbol{s}_1$ and $\boldsymbol{s}_2$ can be written as:

$$\begin{aligned} \boldsymbol{J}\dot{\boldsymbol{s}}_1 &= \boldsymbol{J}\ddot{\tilde{\boldsymbol{q}}}_v + k_1\boldsymbol{J}\dot{\tilde{\boldsymbol{q}}}_v \\ &= \frac{1}{2}\boldsymbol{J}\left(\dot{\tilde{\boldsymbol{q}}}_v^{\times} + \dot{\tilde{q}}_0\boldsymbol{I}_3\right)\tilde{\boldsymbol{\omega}} + \frac{1}{2}\left(\tilde{\boldsymbol{q}}_v^{\times} + \tilde{q}_0\boldsymbol{I}_3\right) \\ &\quad \times \left(-\boldsymbol{C}_r\tilde{\boldsymbol{\omega}} - \boldsymbol{n}_r + \boldsymbol{\varepsilon}_r + \boldsymbol{d}_r\right) + k_1\boldsymbol{J}\dot{\tilde{\boldsymbol{q}}}_{\mathrm{v}} \end{aligned} \tag{31}$$

$$\begin{aligned} m\dot{\boldsymbol{s}}_2 &= m\left(\ddot{\tilde{\boldsymbol{r}}} + k_2\dot{\tilde{\boldsymbol{r}}}\right) \\ &= m\dot{\tilde{\boldsymbol{v}}} - m\boldsymbol{C}_t\dot{\tilde{\boldsymbol{r}}} - m\dot{\boldsymbol{C}}_t\tilde{\boldsymbol{r}} + mk_2\dot{\tilde{\boldsymbol{r}}} \\ &= -m\boldsymbol{C}_t\tilde{\boldsymbol{v}} - m\boldsymbol{n}_t + \boldsymbol{\varepsilon}_t + \boldsymbol{d}_t \\ &\quad - m\boldsymbol{C}_t\dot{\tilde{\boldsymbol{r}}} - m\dot{\boldsymbol{C}}_t\tilde{\boldsymbol{r}} + mk_2\dot{\tilde{\boldsymbol{r}}} \end{aligned} \tag{32}$$

Then, the control laws for attitude and orbit tracking systems can be designed as:

$$\begin{aligned} \boldsymbol{\varepsilon}_r = -2\left(\tilde{\boldsymbol{q}}_v^{\times} + \tilde{q}_0\boldsymbol{I}_3\right)^{-1}\Bigg[&\hat{\beta}_1\frac{\boldsymbol{s}_1 \circ (\boldsymbol{h}_1 \circ \boldsymbol{h}_1)}{2\eta_1} \\ &+ k_3\tanh(\boldsymbol{s}_1) + k_4\boldsymbol{s}_1 + \hat{D}_r\tanh\left(\frac{\boldsymbol{s}_1}{\mu_1}\right)\Bigg] \end{aligned} \tag{33}$$

$$\begin{aligned} \boldsymbol{\varepsilon}_t = &-k_5\tanh(\boldsymbol{s}_2) - k_6\boldsymbol{s}_2 \\ &- \hat{\beta}_2\frac{\boldsymbol{s}_2 \circ (\boldsymbol{h}_2 \circ \boldsymbol{h}_2)}{2\eta_2} - \hat{D}_t\tanh\left(\frac{\boldsymbol{s}_2}{\mu_2}\right) \end{aligned} \tag{34}$$

where $k_i > 0, i = 3, 4, 5, 6$, $\hat{D}_r$, $\hat{D}_t$, $\hat{\beta}_1$ and $\hat{\beta}_2$ are estimations of $\widehat{D}_r$, $\widehat{D}_t$, β_1 and β_2, respectively. Here, $\widehat{D}_r$ and $\widehat{D}_t$ are the upper bound of the lumped disturbance and be denoted in the further discussion.

The derivative of $\hat{D}_r$, $\hat{D}_t$, $\hat{\beta}_1$ and $\hat{\beta}_2$ are denoted as following

$$\dot{\hat{D}}_r = \mathrm{c}_1\left(\|\boldsymbol{s}_1\|\tanh\left(\frac{\|\boldsymbol{s}_1\|}{3\mu_1}\right) - c_5\hat{D}_r\right) \tag{35}$$

$$\dot{\hat{D}}_t = c_2\left(\|\boldsymbol{s}_2\|\tanh\left(\frac{\|\boldsymbol{s}_2\|}{3\mu_2}\right) - c_6\hat{D}_t\right) \tag{36}$$

$$\dot{\hat{\beta}}_1 = c_3\left(\sum_{i=1}^{3}\frac{s_{1i}^2\|\boldsymbol{h}_{1i}\|^2}{2\eta_1} - c_7\hat{\beta}_1\right) \tag{37}$$

$$\dot{\hat{\beta}}_2 = c_4\left(\sum_{i=1}^{3}\frac{s_{2i}^2\|\boldsymbol{h}_{2i}\|^2}{2\eta_2} - c_8\hat{\beta}_2\right) \tag{38}$$

where $c_i > 0, i = 1, 2, \ldots, 4$, $c_j > 1, j = 5, 6, \ldots, 8$.

The definition of estimation errors can be expressed as

$$\tilde{D}_r = \widehat{D}_r - \hat{D}_r \tag{39}$$

$$\tilde{D}_t = \widehat{D}_t - \hat{D}_t \tag{40}$$

$$\tilde{\beta}_1 = \beta_1 - \hat{\beta}_1 \tag{41}$$

$$\tilde{\beta}_2 = \beta_2 - \hat{\beta}_2 \tag{42}$$

Remark 1: In Eqs. (31)-(32), it considers that all actuators work normally. Therefore, the faults coefficients $\boldsymbol{\delta}_r$ and $\boldsymbol{\delta}_t$ in relative dynamics can be expressed as $\boldsymbol{\delta}_r = \boldsymbol{I}_3$ and $\boldsymbol{\delta}_t = \boldsymbol{I}_3$, respectively.

Remark 2: Parameters β_1 and β_2 are the induced norms of the weight matrix, which can effectively reduce the computational complexity.

Theorem 1: Considering the dynamics expressed in Eqs. (2), (3), (23) and (24) under Assumptions 1-3, if the inertia parameters and the mass of the pursuer spacecraft are unknown and the actuators work normally, asymptotic stability of the tracking errors $\tilde{\boldsymbol{q}}_{\mathrm{v}}$ and $\tilde{\boldsymbol{r}}$ will be achieved when the control laws are developed as Eqs. (35)-(38). Additionally, the estimation errors $\tilde{D}_r$, $\tilde{D}_t$, $\tilde{\beta}_1$ and $\tilde{\beta}_2$ are uniformly ultimately bounded.

Proof: The Lyapunov function to clarify the stability of the system is chosen as follows

$$V_1 = \frac{1}{2}\boldsymbol{s}_1^{\mathrm{T}}\boldsymbol{J}\boldsymbol{s}_1 + \frac{1}{2}\boldsymbol{s}_2^{\mathrm{T}}m\boldsymbol{s}_2 + \frac{1}{2c_1}\tilde{D}_r^2$$

$$+\frac{1}{2c_2}\tilde{D}_t^2+\frac{1}{2c_3}\tilde{\beta}_1^2+\frac{1}{2c_4}\tilde{\beta}_2^2 \quad (43)$$

Take the derivative of Eq. (43) and substituting Eqs. (31)-(34) yield

$$\begin{aligned}\dot{V}_1 &= \boldsymbol{s}_1^{\mathrm{T}}\boldsymbol{J}\dot{\boldsymbol{s}}_1+\boldsymbol{s}_2^{\mathrm{T}}m\dot{\boldsymbol{s}}_2+\frac{1}{c_1}\tilde{D}_r\dot{\tilde{D}}_r\\&\quad+\frac{1}{c_2}\tilde{D}_t\dot{\tilde{D}}_t+\frac{1}{c_3}\tilde{\beta}_1\dot{\tilde{\beta}}_1+\frac{1}{c_4}\tilde{\beta}_2\dot{\tilde{\beta}}_2\\&=\boldsymbol{s}_1^{\mathrm{T}}\left(\frac{1}{2}\boldsymbol{J}\left(\dot{\tilde{\boldsymbol{q}}}_v^{\times}+\dot{\tilde{q}}_0\boldsymbol{I}_3\right)\tilde{\boldsymbol{\omega}}+k_1\boldsymbol{J}\dot{\tilde{\boldsymbol{q}}}-\frac{1}{2}\left(\tilde{\boldsymbol{q}}_v^{\times}+\tilde{q}_0\boldsymbol{I}_3\right)\right.\\&\quad\left.\times\left(\boldsymbol{C}_r\tilde{\boldsymbol{\omega}}+\boldsymbol{n}_r\right)\right)+\frac{1}{2}\boldsymbol{s}_1^{\mathrm{T}}\left(\tilde{\boldsymbol{q}}_v^{\times}+\tilde{q}_0\boldsymbol{I}_3\right)\boldsymbol{d}_r\\&\quad+\frac{1}{2}\boldsymbol{s}_1^{\mathrm{T}}\left(\tilde{\boldsymbol{q}}_v^{\times}+\tilde{q}_0\boldsymbol{I}_3\right)\boldsymbol{\varepsilon}_r+\boldsymbol{s}_2^{\mathrm{T}}\left(-m\boldsymbol{C}_t\tilde{\boldsymbol{v}}-m\boldsymbol{n}_t\right.\\&\quad\left.-m\boldsymbol{C}_t\dot{\tilde{\boldsymbol{r}}}-m\dot{\boldsymbol{C}}_t\tilde{\boldsymbol{r}}+mk_2\dot{\tilde{\boldsymbol{r}}}\right)+\boldsymbol{s}_2^{\mathrm{T}}\boldsymbol{d}_t+\boldsymbol{s}_2^{\mathrm{T}}\boldsymbol{\varepsilon}_t\\&\quad-\frac{1}{c_1}\tilde{D}_r\dot{\tilde{D}}_r-\frac{1}{c_2}\tilde{D}_t\dot{\tilde{D}}_t-\frac{1}{c_3}\tilde{\beta}_1\dot{\tilde{\beta}}_1-\frac{1}{c_4}\tilde{\beta}_2\dot{\tilde{\beta}}_2 \quad (44)\end{aligned}$$

Then, it introduces notations $\boldsymbol{H}_1$ and $\boldsymbol{H}_2$ as

$$\begin{aligned}\boldsymbol{H}_1 &= \frac{1}{2}\boldsymbol{J}\left(\dot{\tilde{\boldsymbol{q}}}_v^{\times}+\dot{\tilde{q}}_0\boldsymbol{I}_3\right)\tilde{\boldsymbol{\omega}}+k_1\boldsymbol{J}\dot{\tilde{\boldsymbol{q}}}\\&\quad-\frac{1}{2}\left(\tilde{\boldsymbol{q}}_v^{\times}+\tilde{q}_0\boldsymbol{I}_3\right)\left(\boldsymbol{C}_r\tilde{\boldsymbol{\omega}}+\boldsymbol{n}_r\right) \quad (45)\\\boldsymbol{H}_2 &= -m\boldsymbol{C}_t\tilde{\boldsymbol{v}}-m\boldsymbol{n}_t-m\boldsymbol{C}_t\dot{\tilde{\boldsymbol{r}}}-m\dot{\boldsymbol{C}}_t\tilde{\boldsymbol{r}}+mk_2\dot{\tilde{\boldsymbol{r}}} \quad (46)\end{aligned}$$

By the utilization of MLP algorithm, $\boldsymbol{H}_1$ and $\boldsymbol{H}_2$ is expressed as

$$\boldsymbol{H}_1 = \boldsymbol{W}_1^*\circ\boldsymbol{h}_1+\varepsilon_1 \quad (47)$$
$$\boldsymbol{H}_2 = \boldsymbol{W}_2^*\circ\boldsymbol{h}_2+\varepsilon_2 \quad (48)$$

where $\boldsymbol{W}^* = \left[\boldsymbol{W}_1^*, \boldsymbol{W}_2^*, \boldsymbol{W}_3^*\right]^{\mathrm{T}}$ is the weight matrix; $\boldsymbol{h} = [\boldsymbol{h}_1, \boldsymbol{h}_2, \boldsymbol{h}_3]^{\mathrm{T}}$ expresses the radial basis function vector; ε_1 and ε_2 are the approximation errors satisfying $\varepsilon_i \le \varepsilon_{\mathrm{d}}$, $(i = 1, 2)$ with $\varepsilon_{\mathrm{d}} > 0$.

Substituting Eqs. (45)-(48) into Eq. (44), the following inequality can be derived:

$$\begin{aligned}\dot{V}_1 &= \boldsymbol{s}_1^{\mathrm{T}}\boldsymbol{H}_1+\frac{1}{2}\boldsymbol{s}_1^{\mathrm{T}}\left(\tilde{\boldsymbol{q}}_v^{\times}+\tilde{q}_0\boldsymbol{I}_3\right)\boldsymbol{d}_r+\boldsymbol{s}_2^{\mathrm{T}}\boldsymbol{H}_2+\boldsymbol{s}_2^{\mathrm{T}}\boldsymbol{d}_t\\&\quad+\frac{1}{2}\boldsymbol{s}_1^{\mathrm{T}}\left(\tilde{\boldsymbol{q}}_v^{\times}+\tilde{q}_0\boldsymbol{I}_3\right)\boldsymbol{\varepsilon}_r+\boldsymbol{s}_2^{\mathrm{T}}\boldsymbol{\varepsilon}_t\\&\quad-\frac{1}{c_1}\tilde{D}_r\dot{\tilde{D}}_r-\frac{1}{c_2}\tilde{D}_t\dot{\tilde{D}}_t-\frac{1}{c_3}\tilde{\beta}_1\dot{\tilde{\beta}}_1-\frac{1}{c_4}\tilde{\beta}_2\dot{\tilde{\beta}}_2\\&\le \boldsymbol{s}_1^{\mathrm{T}}\boldsymbol{W}_1^*\circ\boldsymbol{h}_1+\|\boldsymbol{s}_1\|\left(\varepsilon_1+\frac{1}{2}D_r\right)-k_3\|\boldsymbol{s}_1\|\\&\quad-k_4\|\boldsymbol{s}_1\|^2-\boldsymbol{s}_1^{\mathrm{T}}\hat{D}_r\tanh\left(\frac{\boldsymbol{s}_1}{\mu_1}\right)-\hat{\beta}_1\boldsymbol{s}_1^{\mathrm{T}}\frac{\boldsymbol{s}_1\circ(\boldsymbol{h}_1\circ\boldsymbol{h}_1)}{2\eta_1}\\&\quad+\boldsymbol{s}_2^{\mathrm{T}}\boldsymbol{W}_2^*\circ\boldsymbol{h}_2+\|\boldsymbol{s}_2\|(\varepsilon_2+D_t)-k_5\|\boldsymbol{s}_2\|\\&\quad-k_6\|\boldsymbol{s}_2\|^2-\boldsymbol{s}_2^{\mathrm{T}}\hat{D}_t\tanh\left(\frac{\boldsymbol{s}_2}{\mu_2}\right)-\hat{\beta}_2\boldsymbol{s}_2^{\mathrm{T}}\frac{\boldsymbol{s}_2\circ(\boldsymbol{h}_2\circ\boldsymbol{h}_2)}{2\eta_2}\\&\quad-\frac{1}{c_1}\tilde{D}_r\dot{\tilde{D}}_r-\frac{1}{c_2}\tilde{D}_t\dot{\tilde{D}}_t-\frac{1}{c_3}\tilde{\beta}_1\dot{\tilde{\beta}}_1-\frac{1}{c_4}\tilde{\beta}_2\dot{\tilde{\beta}}_2\\&\quad+3\kappa(k_3+k_5) \quad (49)\end{aligned}$$

Here, terms $\boldsymbol{s}_1^{\mathrm{T}}\boldsymbol{W}_1^*\circ\boldsymbol{h}_1$ and $\boldsymbol{s}_2^{\mathrm{T}}\boldsymbol{W}_2^*\circ\boldsymbol{h}_2$ can be expressed as Eq. (50) and Eq. (51), respectively. Moreover, notations $\widehat{D}_r$ and $\widehat{D}_r$ are defined in Eq. (52) and Eq. (53), respectively.

$$\boldsymbol{s}_1^{\mathrm{T}}\boldsymbol{W}_1^*\circ\boldsymbol{h}_1 = [s_{11}, s_{12}, s_{13}]\begin{bmatrix}\boldsymbol{W}_{11}^{*T}\boldsymbol{h}_{11}\\\boldsymbol{W}_{12}^{*T}\boldsymbol{h}_{12}\\\boldsymbol{W}_{13}^{*T}\boldsymbol{h}_{13}\end{bmatrix}=\sum_{i=1}^{3}s_{1i}\boldsymbol{W}_{1i}^{*T}\boldsymbol{h}_{1i} \quad (50)$$

$$\boldsymbol{s}_2^{\mathrm{T}}\boldsymbol{W}_2^*\circ\boldsymbol{h}_2 = [s_{21}, s_{22}, s_{23}]\begin{bmatrix}\boldsymbol{W}_{21}^{*T}\boldsymbol{h}_{21}\\\boldsymbol{W}_{22}^{*T}\boldsymbol{h}_{22}\\\boldsymbol{W}_{23}^{*T}\boldsymbol{h}_{23}\end{bmatrix}=\sum_{i=1}^{3}s_{2i}\boldsymbol{W}_{2i}^{*T}\boldsymbol{h}_{2i} \quad (51)$$

$$\widehat{D}_r = \left(\varepsilon_1+\frac{1}{2}D_r\right) \quad (52)$$

$$\widehat{D}_t = (\varepsilon_2+D_t) \quad (53)$$

In view of Eqs. (50) and (51), Eq. (49) is further derived as:

$$\begin{aligned}\dot{V}_1 &\le \sum_{i=1}^{3}\frac{\beta_1 s_{1i}^2\|\boldsymbol{h}_{1i}\|^2}{2\eta_1}+\widehat{D}_r\|\boldsymbol{s}_1\|-k_3\|\boldsymbol{s}_1\|-k_4\|\boldsymbol{s}_1\|^2\\&\quad-\hat{D}_r\|\boldsymbol{s}_1\|-\sum_{i=1}^{3}\frac{\hat{\beta}_1 s_{1i}^2\|\boldsymbol{h}_{1i}\|^2}{2\eta_1}+3\mu_1\hat{D}_r\kappa\\&\quad+\sum_{i=1}^{3}\frac{\beta_2 s_{2i}^2\|\boldsymbol{h}_{2i}\|^2}{2\eta_2}+\widehat{D}_t\|\boldsymbol{s}_2\|-k_5\|\boldsymbol{s}_2\|-k_6\|\boldsymbol{s}_2\|^2\\&\quad-\hat{D}_t\|\boldsymbol{s}_2\|-\sum_{i=1}^{3}\frac{\hat{\beta}_2 s_{2i}^2\|\boldsymbol{h}_{2i}\|^2}{2\eta_2}+3\mu_2\hat{D}_t\kappa+\frac{3\eta_1}{2}\\&\quad+\frac{3\eta_2}{2}-\frac{1}{c_1}\tilde{D}_r\dot{\tilde{D}}_r-\frac{1}{c_2}\tilde{D}_t\dot{\tilde{D}}_t\\&\quad-\frac{1}{c_3}\tilde{\beta}_1\dot{\tilde{\beta}}_1-\frac{1}{c_4}\tilde{\beta}_2\dot{\tilde{\beta}}_2+3\kappa(k_3+k_5) \quad (54)\end{aligned}$$

where $\eta_1 > 0$, $\eta_2 > 0$ are the design parameters, $\beta_i = \max_{1\le j\le 3}\left\{\left\|\boldsymbol{W}_{ij}^*\right\|^2\right\}$ $(i = 1, 2)$. Substituting Eqs. (35)-(38) into Eq. (54) yields:

$$\begin{aligned}\dot{\boldsymbol{V}}_1 &\le -k_4\|\boldsymbol{s}_1\|^2-k_6\|\boldsymbol{s}_2\|^2+c_5\hat{D}_r\tilde{D}_r+c_6\hat{D}_t\tilde{D}_t\\&\quad+c_7\hat{\beta}_1\tilde{\beta}_1+c_8\hat{\beta}_2\tilde{\beta}_2+3\kappa\left(k_3+k_5+\mu_1\widehat{D}_r+\mu_2\widehat{D}_t\right)\\&\quad+\frac{3}{2}(\eta_1+\eta_2)\\&\le -k_4\|\boldsymbol{s}_1\|^2-k_6\|\boldsymbol{s}_2\|^2-\left(D_r-\hat{D}_r\right)^2-\left(D_t-\hat{D}_t\right)^2\\&\quad-\left(\beta_1-\hat{\beta}_1\right)^2-\left(\beta_2-\hat{\beta}_2\right)^2+\Delta_1\\&\le -\frac{2k_4}{\lambda_{\max}(\boldsymbol{J})}\left(\frac{1}{2}\boldsymbol{s}_1^{\mathrm{T}}\boldsymbol{J}\boldsymbol{s}_1\right)-\frac{2k_6}{m}\left(\frac{1}{2}\boldsymbol{s}_2^{\mathrm{T}}m\boldsymbol{s}_2\right)\\&\quad-2c_1\left(\frac{1}{2c_1}\tilde{D}_r^2\right)-2c_2\left(\frac{1}{2c_2}\tilde{D}^2\right)\\&\quad-2c_3\left(\frac{1}{2c_3}\tilde{\beta}_1^2\right)-2c_4\left(\frac{1}{2c_4}\tilde{\beta}_2^2\right)+\Delta_1\\&= -\rho_1\boldsymbol{V}_1+\Delta_1 \quad (55)\end{aligned}$$

where $\rho_1 = \min\left\{\frac{2k_4}{\lambda_{\max}(\boldsymbol{J})}, \frac{2k_6}{m}, 2c_1, 2c_2, 2c_3, 2c_4\right\}$, $\Delta_1 = 3\kappa\left(k_3 + k_5 + \mu_1\widehat{D}_r + \mu_2\widehat{D}_t\right) + \frac{3}{2}(\eta_1 + \eta_2) + \frac{c_5^2 D_r^2}{4(c_5-1)} + \frac{c_6^2 D_t^2}{4(c_6-1)} + \frac{c_7^2\beta_1^2}{4(c_7-1)} + \frac{c_8^2\beta_2^2}{4(c_8-1)}$.

On the basis of Eq. (55), it proves that $\boldsymbol{s}_1$, $\boldsymbol{s}_2$, $\tilde{D}_r$, $\tilde{D}_t$, $\tilde{\beta}_1$ and $\tilde{\beta}_2$ are uniformly ultimately bounded. Additionally, the sliding mode valuables $\boldsymbol{s}_1$ and $\boldsymbol{s}_2$ will converge to two small regions Θ_1 and Θ_2 as time goes infinite. When the relations $\|\boldsymbol{s}_1\| \le \Theta_1$ and $\|\boldsymbol{s}_2\| \le \Theta_2$ are satisfied, one has

$$\dot{\tilde{q}}_{vi} + k_1\tilde{q}_{vi} = \vartheta_{vi}, |\vartheta_{vi}| \le \Theta_1 \tag{56}$$

$$\dot{\tilde{r}}_i + k_2\tilde{r}_i = \vartheta_{ri}, \vartheta_{ri} \le \Theta_2 \tag{57}$$

Furthermore, the following Lyapunov Function is constructed as

$$V_2 = \frac{1}{2}\tilde{q}_{vi}^2 + \frac{1}{2}r_i^2 \tag{58}$$

In terms of Eqs. (56)-(57), the derivative of V_2 satisfies

$$\begin{aligned}\dot{V}_2 &= \tilde{q}_{vi}\dot{\tilde{q}}_{vi} + r_i\dot{r}_i \\ &\le \tilde{q}_{vi}(\Theta_1 - k_1\tilde{q}_{vi}) + r_i(\Theta_2 - k_2\tilde{r}_i) \\ &= -\left(k_1\tilde{q}_{vi}^2 + k_1\tilde{r}_i^2\right) + \Theta_1\tilde{q}_{vi} + \Theta_2 r_i \\ &\le -\frac{k_1}{2}\tilde{q}_{vi}^2 - \frac{k_2}{2}\tilde{r}_i^2 + \frac{\Theta_1^2 + \Theta_2^2}{2} \\ &\le -\min\{k_1, k_2\}V_2 + \frac{1}{2}\left(\frac{\Theta_1^2}{k_1} + \frac{\Theta_2^2}{k_2}\right)\end{aligned} \tag{59}$$

In addition, the asymptotic stability of tracking errors $\tilde{\boldsymbol{q}}_{\mathrm{v}}$ and $\tilde{\boldsymbol{r}}$ is proved.

Thus, Theorem 1 has been proven.

B. FAULT TOLERANT ATTITUDE CONTROLLER DESIGN

In the basic controller, the actuator failure is not taken into consideration. As a matter of fact, the unexpected and complex failures will occur to the actuators frequently in actual space activities, which will cause severe performance degradation. Therefore, a fault-tolerant control scheme is proposed in this section to improve the system reliability.

Considering the partial loss of actuator effectiveness failures, the sliding mode valuables $\boldsymbol{s}_1$ and $\boldsymbol{s}_2$ satisfy:

$$\begin{aligned}\boldsymbol{J}\dot{\boldsymbol{s}}_1 &= \mathbf{J}\ddot{\tilde{\boldsymbol{q}}}_v + k_1\mathbf{J}\dot{\tilde{\boldsymbol{q}}}_v \\ &= \frac{1}{2}\boldsymbol{J}\left(\dot{\tilde{\boldsymbol{q}}}_v^{\times} + \dot{\tilde{q}}_0\boldsymbol{I}_3\right)\tilde{\boldsymbol{\omega}} + \frac{1}{2}\left(\tilde{\boldsymbol{q}}_v^{\times} + \tilde{q}_0\boldsymbol{I}_3\right) \\ &\quad \times\left(-\boldsymbol{C}_r\tilde{\boldsymbol{\omega}} - \boldsymbol{n}_r + \boldsymbol{\delta}_r\boldsymbol{\varepsilon}_r + \boldsymbol{d}_r\right) + k_1\boldsymbol{J}\dot{\tilde{\boldsymbol{q}}}_v\end{aligned} \tag{60}$$

$$\begin{aligned}m\dot{\boldsymbol{s}}_2 &= m\left(\ddot{\tilde{\boldsymbol{r}}} + k_2\dot{\tilde{\boldsymbol{r}}}\right) \\ &= m\dot{\tilde{\boldsymbol{v}}} - m\boldsymbol{C}_t\dot{\tilde{\boldsymbol{r}}} - m\dot{\boldsymbol{C}}_t\tilde{\boldsymbol{r}} + mk_2\dot{\tilde{\boldsymbol{r}}} \\ &= -m\boldsymbol{C}_t\tilde{\boldsymbol{v}} - m\boldsymbol{n}_t + \boldsymbol{\delta}_t\boldsymbol{\varepsilon}_t + \boldsymbol{d}_t \\ &\quad - m\boldsymbol{C}_t\dot{\tilde{\boldsymbol{r}}} - m\dot{\boldsymbol{C}}_t\tilde{\boldsymbol{r}} + mk_2\dot{\tilde{\boldsymbol{r}}}\end{aligned} \tag{61}$$

Control laws for attitude and orbit tracking systems can be developed as:

$$\boldsymbol{\varepsilon}_r = -2\left(\tilde{\boldsymbol{q}}_v^{\times} + \tilde{q}_0\boldsymbol{I}_3\right)^{-1}(\boldsymbol{\varepsilon}_{r1} + \boldsymbol{\varepsilon}_{r2}) \tag{62}$$

$$\boldsymbol{\varepsilon}_t = -(\boldsymbol{\varepsilon}_{t1} + \boldsymbol{\varepsilon}_{t2}) \tag{63}$$

where

$$\begin{aligned}\boldsymbol{\varepsilon}_{r1} &= \hat{\beta}_1\frac{\boldsymbol{s}_1 \circ (\boldsymbol{h}_1 \circ \boldsymbol{h}_1)}{2\eta_1} + k_3\tanh(\boldsymbol{s}_1) \\ &\quad + k_4\boldsymbol{s}_1 + \hat{D}_r\tanh\left(\frac{\boldsymbol{s}_1}{\mu_1}\right)\end{aligned} \tag{64}$$

$$\boldsymbol{\varepsilon}_{r2} = \hat{\gamma}_r\|\boldsymbol{\varepsilon}_{r1}\|\tanh\left(\frac{\|\boldsymbol{\varepsilon}_{r1}\|\boldsymbol{s}_1}{\mu_3}\right) \tag{65}$$

$$\begin{aligned}\boldsymbol{\varepsilon}_{t1} &= k_5\tanh(\boldsymbol{s}_2) + k_6\boldsymbol{s}_2 \\ &\quad + \hat{\beta}_2\frac{\boldsymbol{s}_2 \circ (\boldsymbol{h}_2 \circ \boldsymbol{h}_2)}{2\eta_2} + \hat{D}_t\tanh\left(\frac{\boldsymbol{s}_2}{\mu_2}\right)\end{aligned} \tag{66}$$

$$\boldsymbol{\varepsilon}_{t2} = \hat{\gamma}_t\|\boldsymbol{\varepsilon}_{t1}\|\tanh\left(\frac{\|\boldsymbol{\varepsilon}_{t1}\|\boldsymbol{s}_2}{\mu_4}\right) \tag{67}$$

with $k_i > 0$, $i = 3, 4, 5, 6$.

The definition of $\hat{\gamma}_r$ and $\hat{\gamma}_r$ are given as:

$$\dot{\hat{\gamma}}_r = c_9\left(\|\boldsymbol{\varepsilon}_{r1}\|\|\boldsymbol{s}_1\|\tanh\left(\frac{\|\boldsymbol{\varepsilon}_{r1}\|\|\boldsymbol{s}_1\|}{3\mu_3}\right) - k_7\hat{\gamma}_r\right) \tag{68}$$

$$\dot{\hat{\gamma}}_t = c_{10}\left(\|\boldsymbol{\varepsilon}_{t1}\|\|\boldsymbol{s}_2\|\tanh\left(\frac{\|\boldsymbol{\varepsilon}_{t1}\|\|\boldsymbol{s}_2\|}{3\mu_4}\right) - k_8\hat{\gamma}_t\right) \tag{69}$$

where c_9, c_{10}, k_7, k_8 are constants satisfying $c_9 > 0$, $c_{10} > 0$, $k_7 > 1$, $k_8 > 1$, $\gamma_r = \frac{1-\theta_r}{\theta_r}$ and $\gamma_t = \frac{1-\theta_t}{\theta_t}$.

Definitions of estimation errors are expressed as

$$\tilde{\gamma}_r = \gamma_r - \hat{\gamma}_r \tag{70}$$

$$\tilde{\gamma}_t = \gamma_t - \hat{\gamma}_t \tag{71}$$

Remark 3: Considering the partial loss of actuator effectiveness failures, the faults coefficients $\boldsymbol{\delta}_r$ and $\boldsymbol{\delta}_t$ in relative dynamics can be expressed as $\boldsymbol{\delta}_r = \mathrm{diag}\{\delta_{r1}, \delta_{r2}, \delta_{r3}\}$ and $\boldsymbol{\delta}_t = \mathrm{diag}\{\delta_{t1}, \delta_{t2}, \delta_{t3}\}$ with $0 < \theta_r < \delta_{ri} \le 1, 0 < \theta_t < \delta_{ti} \le 1, i = 1, 2, 3$.

Theorem 2: Considering the dynamics expressed in Eqs. (2), (3), (23) and (24) under Assumptions 1-3, if the inertia parameters and the mass of the pursuer spacecraft are unknown, the asymptotic stability of tracking errors $\tilde{\boldsymbol{q}}_{\mathrm{v}}$ and $\tilde{\boldsymbol{r}}$ will be obtained when the control laws are designed as Eqs. (35)-(38) and (68)-(69) even in the presence of partial loss of actuator effectiveness failures. Additionally, estimation errors $\tilde{D}_r$, $\tilde{D}_t$, $\tilde{\beta}_1$ and $\tilde{\beta}_2$ are uniformly ultimately bounded.

Proof: In order to clarify the stability of the entire system, the Lyapunov Function can be designed as:

$$\begin{aligned}V_3 &= \frac{1}{2}\boldsymbol{s}_1^{\mathrm{T}}\boldsymbol{J}\boldsymbol{s}_1 + \frac{1}{2}\boldsymbol{s}_2^{\mathrm{T}}m\boldsymbol{s}_2 + \frac{1}{2c_1}\tilde{D}_r^2 + \frac{1}{2c_2}\tilde{D}_t^2 \\ &\quad + \frac{1}{2c_3}\tilde{\beta}_1^2 + \frac{1}{2c_4}\tilde{\beta}_2^2 + \frac{\theta_r}{2c_9}\tilde{\gamma}_r^2 + \frac{\theta_t}{2c_{10}}\tilde{\gamma}_t^2\end{aligned} \tag{72}$$

Upon utilizing Eq. (60) and Eq. (61), the derivative of $\boldsymbol{V}_3$ can be obtained as follows

$$\begin{aligned}\dot{V}_3 &= \boldsymbol{s}_1^{\mathrm{T}}\boldsymbol{J}\dot{\boldsymbol{s}}_1 + \boldsymbol{s}_2^{\mathrm{T}}m\dot{\boldsymbol{s}}_2 + \frac{1}{c_1}\tilde{D}_r\dot{\tilde{D}}_r + \frac{1}{c_2}\tilde{D}_t\dot{\tilde{D}}_t \\ &\quad + \frac{1}{c_3}\tilde{\beta}_1\dot{\tilde{\beta}}_1 + \frac{1}{c_4}\tilde{\beta}_2\dot{\tilde{\beta}}_2 + \frac{\theta_r}{c_9}\tilde{\gamma}_r\dot{\tilde{\gamma}}_r + \frac{\theta_t}{c_{10}}\tilde{\gamma}_t\dot{\tilde{\gamma}}_t\end{aligned}$$

$$
\begin{aligned}
&= \boldsymbol{s}_1^{\mathrm{T}}\left(\frac{1}{2}\boldsymbol{J}\left(\dot{\tilde{\boldsymbol{q}}}_v^{\times}+\dot{\tilde{q}}_0\boldsymbol{I}_3\right)\tilde{\boldsymbol{\omega}}+\frac{1}{2}\left(\tilde{\boldsymbol{q}}_v^{\times}+\tilde{q}_0\boldsymbol{I}_3\right)\right.\\
&\quad\left.\times\left(-\boldsymbol{C}_r\tilde{\boldsymbol{\omega}}-\boldsymbol{n}_r+\boldsymbol{\delta}_r\boldsymbol{\varepsilon}_r+\boldsymbol{d}_r\right)+k_1\boldsymbol{J}\dot{\tilde{\boldsymbol{q}}}_v\right.\\
&\quad+\boldsymbol{s}_2^{\mathrm{T}}\left(-m\boldsymbol{C}_t\tilde{\boldsymbol{v}}-m\boldsymbol{n}_t+\boldsymbol{\delta}_t\boldsymbol{\varepsilon}_t+\boldsymbol{d}_t-m\boldsymbol{C}_t\dot{\tilde{\boldsymbol{r}}}\right.\\
&\quad\left.-m\dot{\boldsymbol{C}}_t\tilde{\boldsymbol{r}}+mk_2\dot{\tilde{\boldsymbol{r}}}\right)+\frac{1}{c_1}\tilde{D}_r\dot{\tilde{D}}_r+\frac{1}{c_2}\tilde{D}_t\dot{\tilde{D}}_t\\
&\quad+\frac{1}{c_3}\tilde{\beta}_1\dot{\tilde{\beta}}_1+\frac{1}{c_4}\tilde{\beta}_2\dot{\tilde{\beta}}_2+\frac{\theta_r}{c_9}\tilde{\gamma}_r\dot{\tilde{\gamma}}_r+\frac{\theta_t}{c_{10}}\tilde{\gamma}_t\dot{\tilde{\gamma}}_t \qquad (73)
\end{aligned}
$$

Combining Eqs. (45)-(48), it follows that

$$
\begin{aligned}
\dot{V}_3 \le\ & \boldsymbol{s}_1^{\mathrm{T}}\boldsymbol{W}_1^{*}\circ\boldsymbol{h}_1+\|\boldsymbol{s}_1\|\widehat{D}_r+\|\boldsymbol{s}_1\|(1-\theta_r)\|\boldsymbol{\varepsilon}_{r1}\|\\
&-\theta_r\hat{\gamma}_r\|\boldsymbol{\varepsilon}_{r1}\|\boldsymbol{s}_1^{\mathrm{T}}\tanh\left(\frac{\|\boldsymbol{\varepsilon}_{r1}\|\boldsymbol{s}_1}{\mu_3}\right)-k_4\|\boldsymbol{s}_1\|^2\\
&-k_3\tanh(\boldsymbol{s}_1)+\boldsymbol{s}_2^{\mathrm{T}}\boldsymbol{W}_2^{*}\circ\boldsymbol{h}_2+\|\boldsymbol{s}_2\|\widehat{D}_t\\
&+\|\boldsymbol{s}_2\|(1-\theta_t)\|\boldsymbol{\varepsilon}_{t1}\|-\theta_t\hat{\gamma}_t\|\boldsymbol{\varepsilon}_{t1}\|\boldsymbol{s}_2^{\mathrm{T}}\tanh\left(\frac{\|\boldsymbol{\varepsilon}_{t1}\|\boldsymbol{s}_2}{\mu_4}\right)\\
&-k_6\|\boldsymbol{s}_2\|^2-k_5\tanh(\boldsymbol{s}_2)-\hat{D}_r\boldsymbol{s}_1^{\mathrm{T}}\tanh\left(\frac{\boldsymbol{s}_1}{\mu_1}\right)\\
&-\sum_{i=1}^{3}\frac{\hat{\beta}_1 s_{1i}^2\|\boldsymbol{h}_{1i}\|^2}{2\eta_1}-\hat{D}_t\boldsymbol{s}_2^{\mathrm{T}}\tanh\left(\frac{\boldsymbol{s}_2}{\mu_2}\right)\\
&-\sum_{i=1}^{3}\frac{\hat{\beta}_2 s_{2i}^2\|\boldsymbol{h}_{2i}\|^2}{2\eta_2}-\frac{1}{c_1}\tilde{D}_r\dot{\tilde{D}}_r-\frac{1}{c_2}\tilde{D}_t\dot{\tilde{D}}_t-\frac{1}{c_3}\tilde{\beta}_1\dot{\tilde{\beta}}_1\\
&-\frac{1}{c_4}\tilde{\beta}_2\dot{\tilde{\beta}}_2-\frac{\theta_r}{c_9}\tilde{\gamma}_r\dot{\tilde{\gamma}}_r-\frac{\theta_t}{c_{10}}\tilde{\gamma}_t\dot{\tilde{\gamma}}_t \qquad (74)
\end{aligned}
$$

Substituting Eqs. (50), (51) into Eq. (74), the inequality can be further written as follows:

$$
\begin{aligned}
&\dot{V}_3\\
&\le\sum_{i=1}^{3}\frac{\beta_1 s_{1i}^2\|\boldsymbol{h}_{1i}\|^2}{2\eta_1}+\frac{3\eta_1}{2}+\widehat{D}_r\|\boldsymbol{s}_1\|\\
&\quad+\|\boldsymbol{s}_1\|(1-\theta_r)\|\boldsymbol{\varepsilon}_{r1}\|-\theta_r\hat{\gamma}_r\|\boldsymbol{\varepsilon}_{r1}\|\boldsymbol{s}_1^{\mathrm{T}}\tanh\left(\frac{\|\boldsymbol{\varepsilon}_{r1}\|\boldsymbol{s}_1}{\mu_3}\right)\\
&\quad-k_3\|\boldsymbol{s}_1\|-k_4\|\boldsymbol{s}_1\|^2-\hat{D}_r\|\boldsymbol{s}_1\|+3\mu_1\hat{D}_r\kappa\\
&\quad-\sum_{i=1}^{3}\frac{\hat{\beta}_1 s_{1i}^2\|\boldsymbol{h}_{1i}\|^2}{2\eta_1}+\sum_{i=1}^{3}\frac{\beta_2 s_{2i}^2\|\boldsymbol{h}_{2i}\|^2}{2\eta_2}+\frac{3\eta_2}{2}+\widehat{D}_t\|\boldsymbol{s}_2\|\\
&\quad+\|\boldsymbol{s}_2\|(1-\theta_t)\|\boldsymbol{\varepsilon}_{t1}\|-\theta_t\hat{\gamma}_t\|\boldsymbol{\varepsilon}_{t1}\|\boldsymbol{s}_2^{\mathrm{T}}\tanh\left(\frac{\|\boldsymbol{\varepsilon}_{t1}\|\boldsymbol{s}_2}{\mu_4}\right)\\
&\quad-k_5\|\boldsymbol{s}_2\|-k_6\|\boldsymbol{s}_2\|^2-\hat{D}_t\|\boldsymbol{s}_2\|+3\mu_2\hat{D}_t\kappa\\
&\quad-\sum_{i=1}^{3}\frac{\hat{\beta}_2 s_{2i}^2\|\boldsymbol{h}_{2i}\|^2}{2\eta_2}-\frac{1}{c_1}\tilde{D}_r\dot{\tilde{D}}_r-\frac{1}{c_2}\tilde{D}_t\dot{\tilde{D}}_t-\frac{1}{c_3}\tilde{\beta}_1\dot{\tilde{\beta}}_1\\
&\quad-\frac{1}{c_4}\tilde{\beta}_2\dot{\tilde{\beta}}_2-\frac{\theta_r}{c_9}\tilde{\gamma}_r\dot{\tilde{\gamma}}_r-\frac{\theta_t}{c_{10}}\tilde{\gamma}_t\dot{\tilde{\gamma}}_t+3\kappa(k_3+k_5) \qquad (75)
\end{aligned}
$$

In terms of the control laws expressed as Eqs. (35)-(38) and (68)-(69), one has

$$
\begin{aligned}
\dot{V}_3 \le\ & -k_4\|\boldsymbol{s}_1\|^2-k_6\|\boldsymbol{s}_2\|^2+c_5\hat{D}_r\tilde{D}_r+c_6\hat{D}_t\tilde{D}_t\\
&+c_7\hat{\beta}_1\tilde{\beta}_1+c_8\hat{\beta}_2\tilde{\beta}_2+k_7\theta_r\hat{\gamma}_r\tilde{\gamma}_r+k_8\theta_t\hat{\gamma}_t\tilde{\gamma}_t\\
&+3\tilde{D}_r\mu_1\kappa+3\tilde{D}_t\mu_2\kappa+\|\boldsymbol{s}_1\|(1-\theta_r)\|\boldsymbol{\varepsilon}_{r1}\|\\
&-\theta_r\hat{\gamma}_r\|\boldsymbol{\varepsilon}_{r1}\|\|\boldsymbol{s}_1\|-\theta_r\tilde{\gamma}_r\|\boldsymbol{\varepsilon}_{r1}\|\|\boldsymbol{s}_1\|+3\mu_3\kappa\theta_r\tilde{\gamma}_r\\
&+\|\boldsymbol{s}_2\|(1-\theta_t)\|\boldsymbol{\varepsilon}_{t1}\|-\theta_t\hat{\gamma}_t\|\boldsymbol{\varepsilon}_{t1}\|\|\boldsymbol{s}_2\|\\
&-\theta_t\tilde{\gamma}_t\|\boldsymbol{\varepsilon}_{t1}\|\|\boldsymbol{s}_2\|+3\mu_4\kappa\theta_t\tilde{\gamma}_t+3\kappa\left(k_3+k_5+\mu_1\hat{D}_r\right.\\
&\left.+\mu_2\hat{D}_t+\theta_r\hat{\gamma}_r\mu_3+\theta_t\hat{\gamma}_t\mu_4\right)+\frac{3\eta_1}{2}+\frac{3\eta_2}{2}\\
=\ & -k_4\|\boldsymbol{s}_1\|^2-k_6\|\boldsymbol{s}_2\|^2-\left(D_r-\hat{D}_r\right)^2\\
&-\left(D_t-\hat{D}_t\right)^2-\left(\beta_1-\hat{\beta}_1\right)^2-\left(\beta_2-\hat{\beta}_2\right)^2\\
&-\theta_r\left(\gamma_r-\hat{\gamma}_r\right)^2-\theta_t\left(\gamma_t-\hat{\gamma}_t\right)^2+\Delta_3 \qquad (76)
\end{aligned}
$$

where $\Delta_3 = 3\kappa\left(k_3+k_5+\mu_1\widehat{D}_r+\mu_2\widehat{D}_t+\theta_r\gamma_r\mu_3+\theta_t\gamma_t\mu_4\right)+\frac{3\eta_1}{2}+\frac{3\eta_2}{2}+\frac{c_5^2D_r^2}{4(c_5-1)}+\frac{c_6^2D_t^2}{4(c_6-1)}+\frac{c_7^2\beta_1^2}{4(c_7-1)}+\frac{c_8^2\beta_2^2}{4(c_8-1)}+\frac{\theta_r k_7^2\gamma_r^2}{4(k_7-1)}+\frac{\theta_t k_8^2\gamma_t^2}{4(k_8-1)}$.

The inequality can be further derived as follows

$$
\begin{aligned}
\dot{V}_3 &\le -\frac{2k_4}{\lambda_{\max}(\boldsymbol{J})}\left(\frac{1}{2}\boldsymbol{s}_1^{\mathrm{T}}\boldsymbol{J}\boldsymbol{s}_1\right)-\frac{2k_6}{m}\left(\frac{1}{2}\boldsymbol{s}_2^{\mathrm{T}}m\boldsymbol{s}_2\right)\\
&\quad-2c_1\left(\frac{1}{2c_1}\tilde{D}^2\right)-2c_2\left(\frac{1}{2c_2}\tilde{D}^2\right)\\
&\quad-2c_3\left(\frac{1}{2c_3}\tilde{\beta}_1^2\right)-2c_4\left(\frac{1}{2c_4}\tilde{\beta}_2^2\right)\\
&\quad-2c_9\left(\frac{\theta_r}{2c_9}\tilde{\gamma}_r^2\right)-2c_{10}\left(\frac{\theta_t}{2c_{10}}\tilde{\gamma}_t^2\right)+\Delta_3\\
&\le -\rho_3 V_3+\Delta_3 \qquad (77)
\end{aligned}
$$

where $\rho_3=\min\left\{\frac{2k_4}{\lambda_{\max}(\boldsymbol{J})},\frac{2k_6}{m},2c_1,2c_2,2c_3,2c_4,2c_9,2c_{10}\right\}$.

Basing on Eq. (77), it proves that $\boldsymbol{s}_1,\boldsymbol{s}_2,\tilde{D}_r,\tilde{D}_t,\tilde{\beta}_1,\tilde{\beta}_2,\tilde{\gamma}_r,\tilde{\gamma}_t$ will coverage to a bounded region of Δ_3 with asymptotic stability. Similar to the analysis in Theorem 1, we can conclude that $\|\boldsymbol{s}_1\|\le\Theta_3$ and $\|\boldsymbol{s}_2\|\le\Theta_4$ will be achieved and the asymptotic stability of the tracking errors $\tilde{\boldsymbol{q}}_{\mathrm{v}}$ and $\tilde{\boldsymbol{r}}$ can also be proved. Here, Θ_3 and Θ_4 are positive constants.

Remark 4: There are many control parameters in the proposed controllers. The selection of these parameters is determined by the control performance. To be more specific, parameters k_3, k_4, k_5 and k_6 are utilized to ensure finite-time stability and disturbance rejection capability. By increasing these four terms, convergence time of the close system will be reduced and control accuracy can be improved considerably. Estimation errors mainly depend on the parameters $c_i, i=1,2,\ldots,10$. In a word, the control performance is decided by these control parameters and in turn, control performance gives the principle of the selection of these parameters.

Remark 5: State constraints are essential in consideration of the system safety, especially for the rendezvous missions of spacecraft. In [30], an effective control method is proposed to deal with state constraints for a class of underactuated systems. This constrained method can be applied for many practical systems. However, it cannot be utilized in this paper directly, since sliding mode method is adopted to develop

TABLE 1. Orbit and spacecraft information [22].

Parameter	Value	Unit
Gravitational constant, μ	6.371	km
Eccentricity, e	0.3	—
Radius of the Earth, R_E	6371	km
Perigee altitude, r_{pa}	400	km
Initial true anomaly, $v(0)$	10	degrees
Inertial matrix, $\boldsymbol{J}$	$\mathrm{diag}(20,20,15)$	$\mathrm{kg}\cdot\mathrm{m}^2$
Inertial matrix, $\boldsymbol{J}_t$	$\mathrm{diag}(26,16,21)$	$\mathrm{kg}\cdot\mathrm{m}^2$
Mass, m	90	kg
Mass, m_t	150	kg

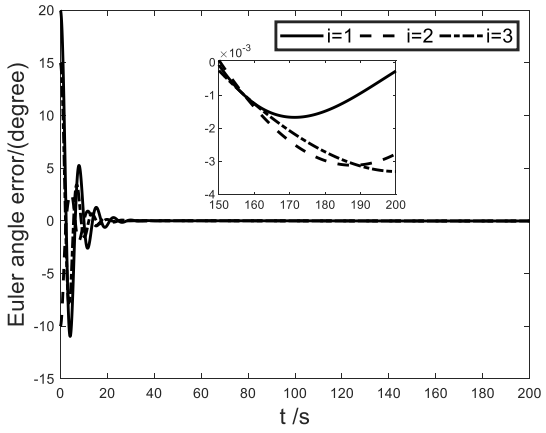

FIGURE 1. Relative angles.

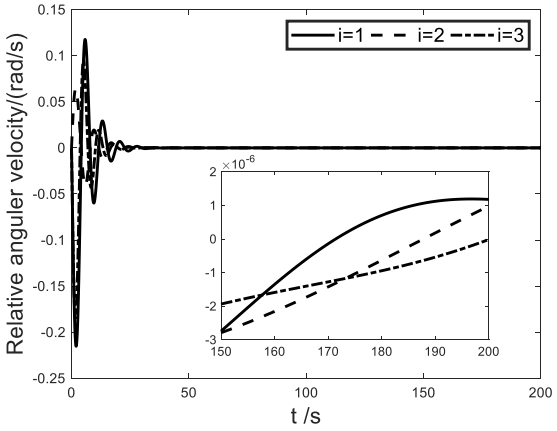

FIGURE 2. Relative angular velocities.

controller here. It is our future work to extend the methods in [30] for spacecraft rendezvous missions.

IV. SPACECRAFT MODEL AND PRELIMINARIES

This section completes numerical simulations to validate the effectiveness and advantage of the developed control strategies. In the simulation scenarios, a pursuer spacecraft is forced to rendezvous with the target spacecraft in an elliptical orbit. Detailed information about the orbit and these two spacecrafts is presented in the following table.

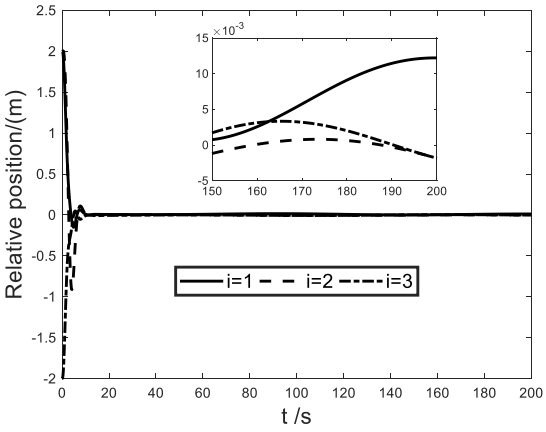

FIGURE 3. Relative position.

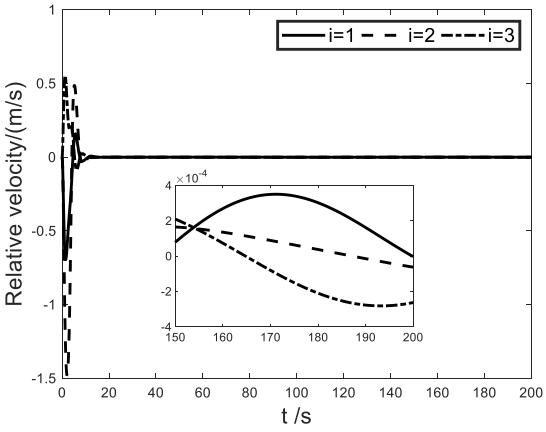

FIGURE 4. Relative velocity.

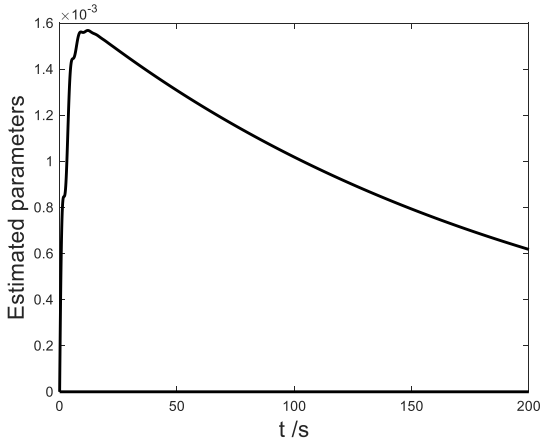

FIGURE 5. The estimated parameter $\hat{D}_r$.

The target spacecraft is supposed to service with the following position:

$$\boldsymbol{r}_t = [r_t, 0, 0]^{\mathrm{T}}, \quad r_t = \frac{a\left(1-e^2\right)}{1+e\cos v}$$

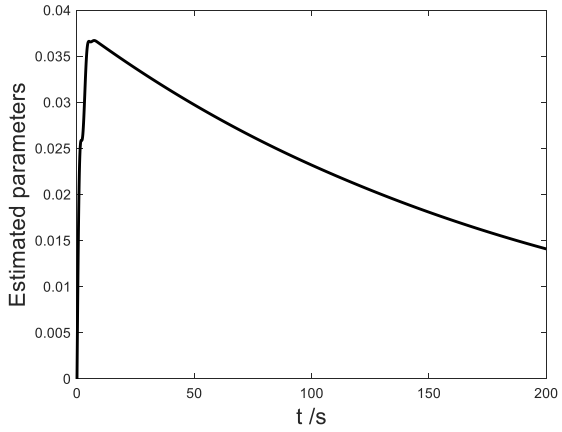

FIGURE 6. The estimated parameter $\hat{D}_t$.

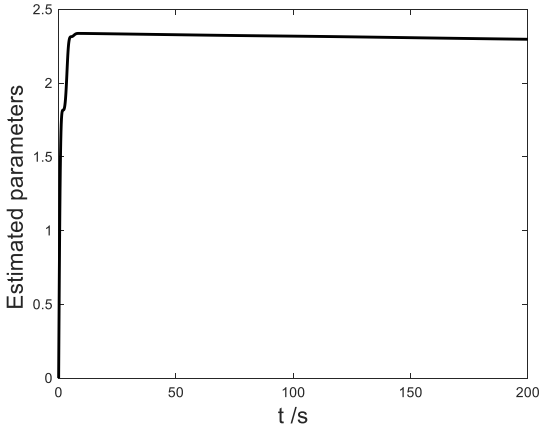

FIGURE 8. The estimated parameter $\hat{\beta}_t$.

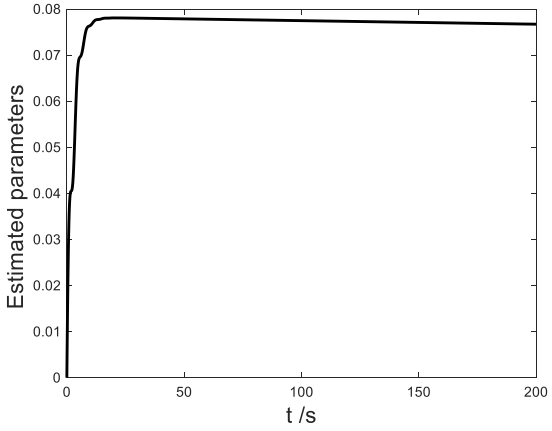

FIGURE 7. The estimated parameter $\hat{\beta}_r$.

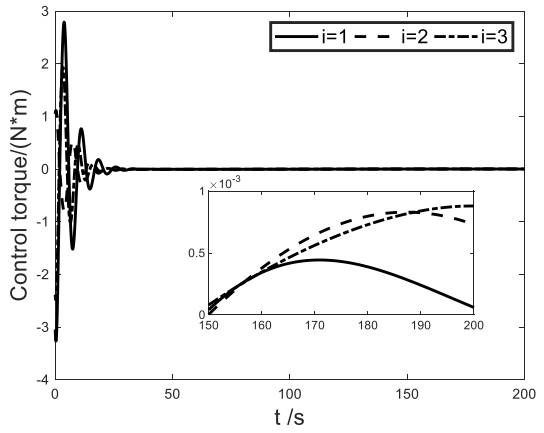

FIGURE 9. The control torque τ.

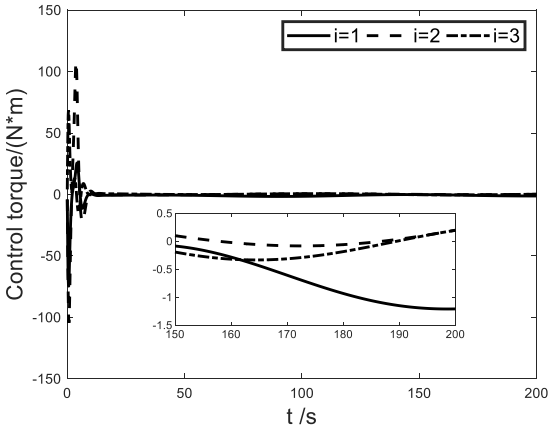

FIGURE 10. The control torque f.

where $a = R_E + \frac{r_{pa}}{1-e}$ denotes the semimajor axis. The parameter v is expressed as follows:

$$\dot{v} = \frac{n\left(1+e\cos v\right)^2}{\left(1-e^2\right)^{\frac{3}{2}}}, \quad \ddot{v} = \frac{2n^2 e\left(1+e\cos v\right)^3 \sin v}{\left(1-e^2\right)^3}$$

where $n = \sqrt{u/a^3}$. For the pursuer spacecraft, its rendezvous position is expressed as $\boldsymbol{\delta}_t = [0, 5, 0]^{\mathrm{T}}$ in the target's body coordinate frame. The angular velocity of the target and the external disturbances are given as:

$$\boldsymbol{\tau}_d = 0.02 \times \left(1+\cos\left(\frac{\pi}{150}t\right)+\sin\left(\frac{\pi}{150}t\right)\right)[1;\,1;\,1]^{\mathrm{T}}\mathrm{N}\cdot\mathrm{m}$$

$$\boldsymbol{f}_d = 0.05 \times \left(1+\cos\left(\frac{\pi}{150}t\right)+\sin\left(\frac{\pi}{150}t\right)\right)[1;\,1;\,1]^{\mathrm{T}}\mathrm{N}\cdot\mathrm{m}$$

The initial states is set as: the initial Euler angle error is $\Theta(0) = [19.9984 - 9.9987\ 15.0050]^{\mathrm{T}}$ deg, $\tilde{\boldsymbol{\omega}} = [000]^{\mathrm{T}}$, $\tilde{\boldsymbol{r}}(0) = [2,2,-2]^{\mathrm{T}}$, $\tilde{\boldsymbol{v}}(0) = [000]^{\mathrm{T}}$.

A. SIMULATION RESULTS OF THE BASIC CONTROLLER

For the first controller, we take the following parameters: $k_1 = 2, k_2 = 1, k_3 = 0.05, k_4 = 4, k_5 = 0.1, k_6 = 2, \eta_1 = 0.5, \eta_2 = 0.5, \mu_1 = 1, \mu_2 = 1, c_1 = 0.005, c_2 = 0.005, c_3 = 0.01, c_4 = 0.001, c_5 = 1, c_6 = 1, c_7 = 0.1, c_8 = 0.1$. Then, the numerical simulation results of the first controller are presented as Figs. 1-10. Fig. 1∼Fig. 4 are the results of the relative angular, relative velocity, relative position, and relative velocity, respectively, which reveal that the target spacecraft could be tracked by the pursuer spacecraft within 20S. It is noteworthy that

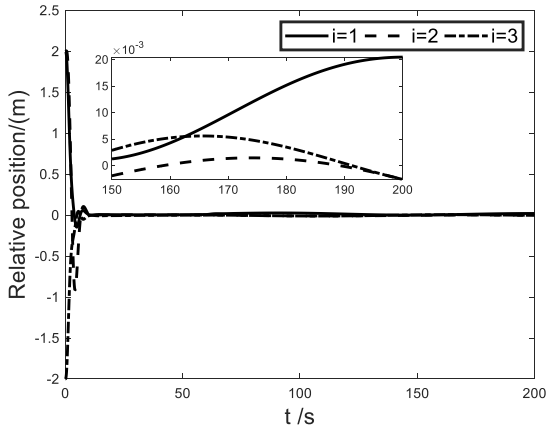

FIGURE 11. Relative angles.

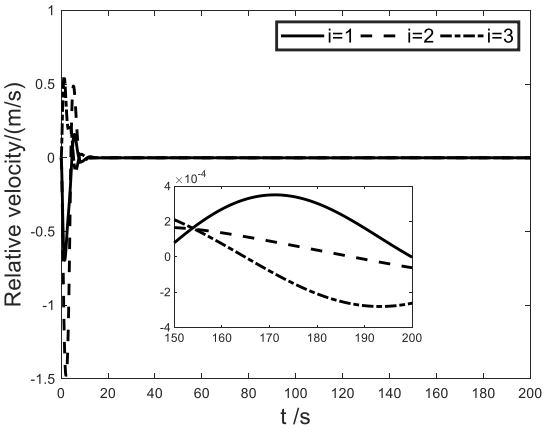

FIGURE 14. Relative velocity.

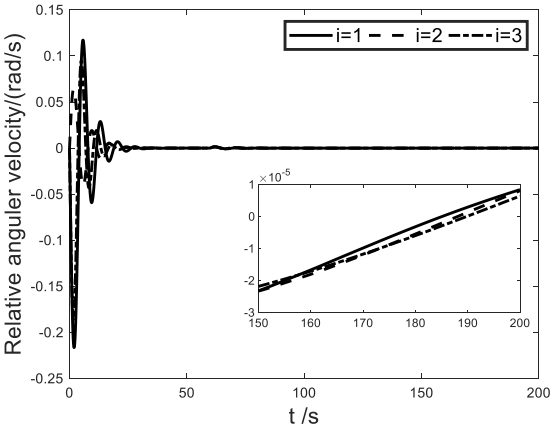

FIGURE 12. Relative angular velocities.

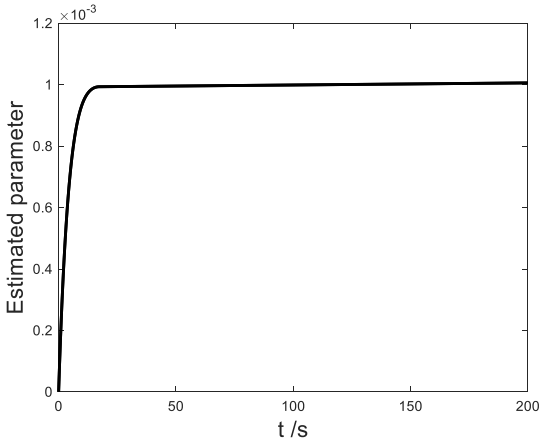

FIGURE 15. The estimated parameter $\hat{D}_r$.

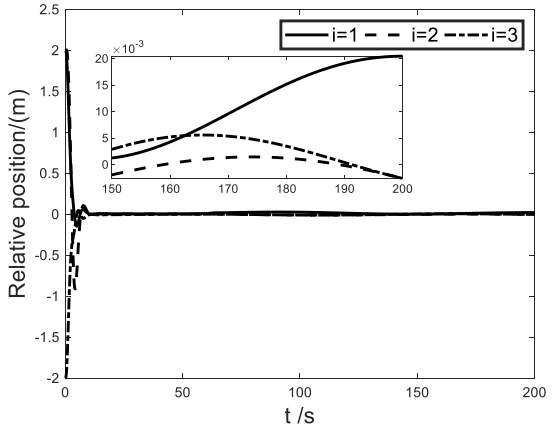

FIGURE 13. Relative position.

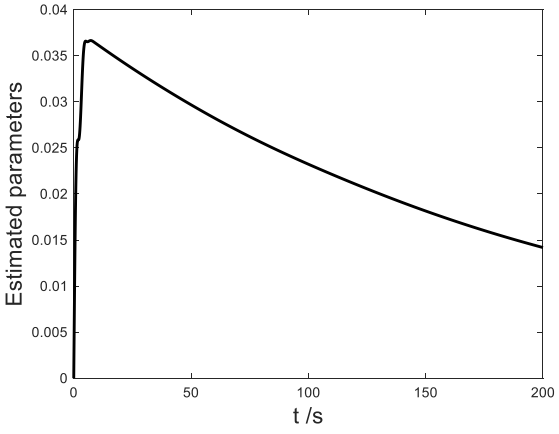

FIGURE 16. The estimated parameter $\hat{D}_t$.

i represents the ith channel of the spacecraft. Figs. 5∼8 are the corresponding estimations of unknown parameters. Observing these results, one can find that the estimated parameters are bounded. Figs. 9∼10 are the control torques of the proposed controllers.

B. SIMULATION RESULTS OF THE FAULT-TOLERANT CONTROLLER

In the case of actuator fault, the fault coefficients are given as: $\delta_{ri} = \begin{cases} 1 \; if \; t < 60 \\ 0.6 \; else \end{cases}$, $\delta_{ti} = \begin{cases} 1 \; if \; t < 60 \\ 0.6 \; else \end{cases}$, $i = 1, 2, 3.$

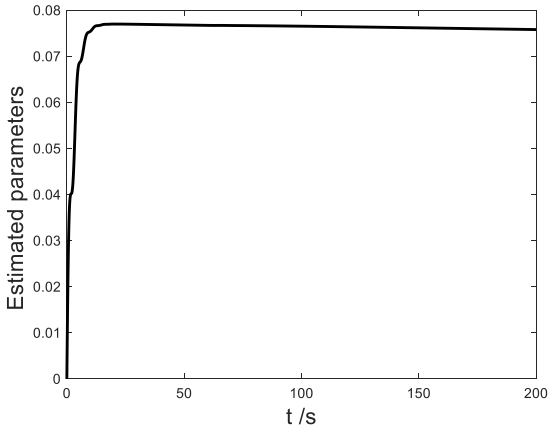

FIGURE 17. The estimated parameter $\hat{\beta}_r$.

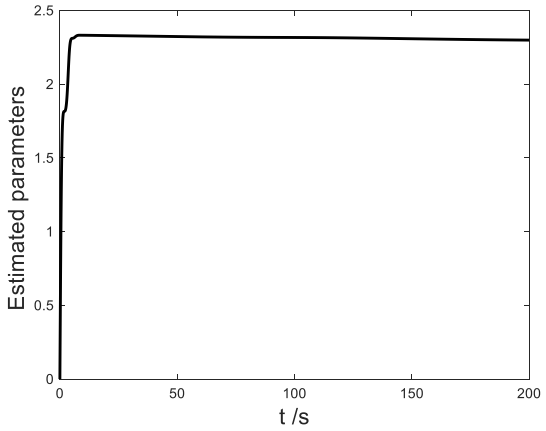

FIGURE 18. The estimated parameter $\hat{\beta}_t$.

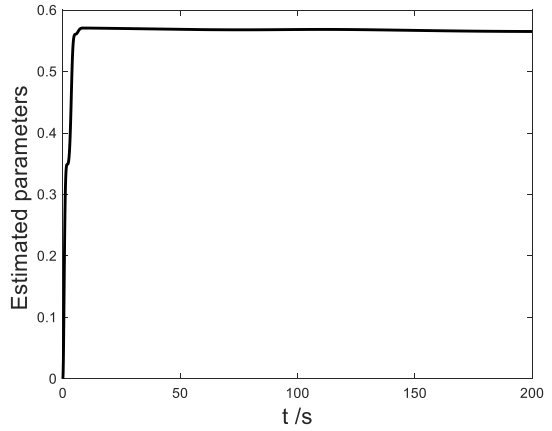

FIGURE 19. The estimated parameter $\hat{\gamma}_r$.

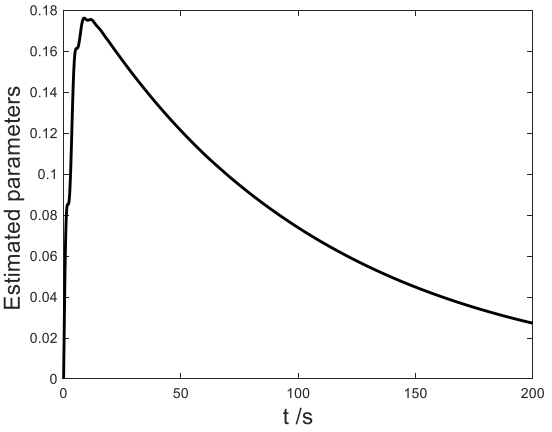

FIGURE 20. The estimated parameter $\hat{\gamma}_t$.

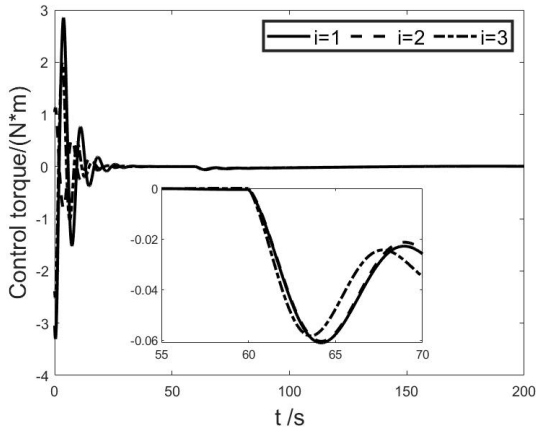

FIGURE 21. The control torque τ.

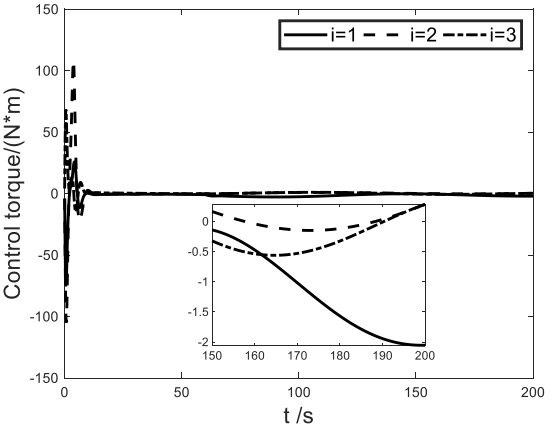

FIGURE 22. The control torque f.

The control parameters are given as: $k_1 = 2$, $k_2 = 1$, $k_3 = 0.05$, $k_4 = 4$, $k_5 = 0.1$, $k_6 = 2$, $k_7 = 0.1$, $k_8 = 0.1$, $\eta_1 = 0.5$, $\eta_2 = 0.5$, $\mu_1 = 1$, $\mu_2 = 1$, $c_1 = 0.005$, $c_2 = 0.005$, $c_3 = 0.01$, $c_4 = 0.001$, $c_5 = 1$, $c_6 = 1$, $c_7 = 0.1$, $c_8 = 0.1$, $c_9 = 0.1$, $c_{10} = 0.001$. The validity has been shown by the corresponding simulation results in Figs. 11∼22, in which the tracking errors are stabilized within 20s and the estimated parameters are bounded. Observing the presented results, one can conclude that the target spacecraft can still be tracked by the pursuer spacecraft even in the presence of the actuator faults.

To better show the superiority of this paper, the second controller in [34] is adopted under the same actuator faults

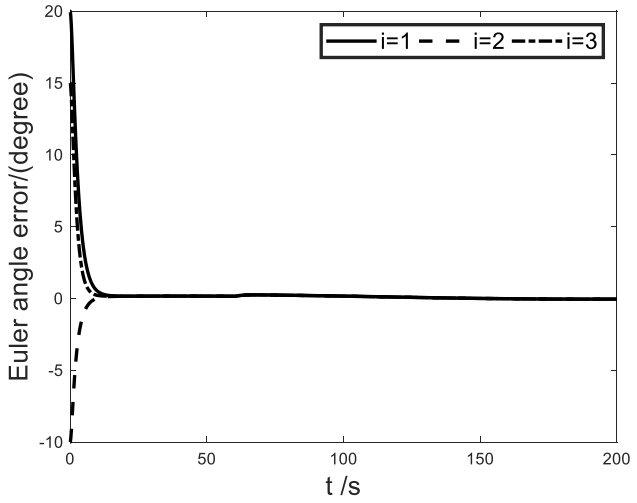

FIGURE 23. Relative attitude under the second controller in [34].

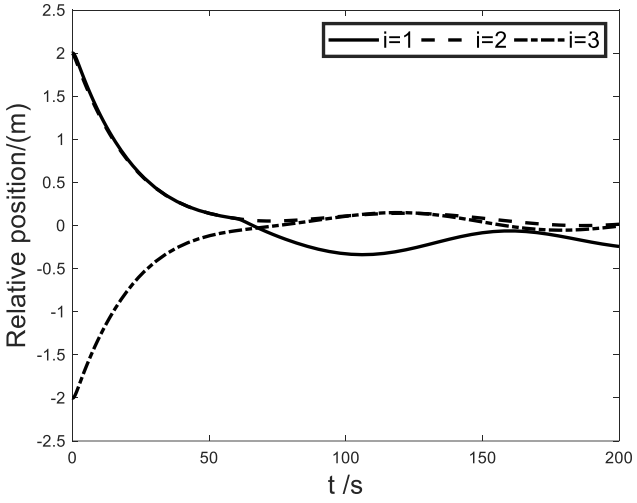

FIGURE 24. Relative position under the second controller in [34].

and external disturbances as that in case B. Figs. 23-24 are the simulation results of this controller. Obviously, actuator faults have little effect on the relative attitude. However, relative positions are significantly affected by this kind of faults. If fault-tolerant design is not taken into consideration, the relative position will not converge to zero, which implies that the rendezvous maneuver will fail. Consequently, actuator faults must be properly dealt with during rendezvous maneuver missions.

V. CONCLUSION

This paper presents two novel robust control strategies for spacecraft rendezvous maneuver based on SMC and Neuro Networks. Upon using the MLP algorithm, the uncertain system dynamics can be estimated with low complexity. The fault-tolerant control scheme could improve the reliability of the spacecraft when the tracking mission is performed during the rendezvous maneuver. Hyperbolic tangent function is introduced into the control law to avoid the chattering problem. Finally, numerical simulation results show that these two methods can not only accomplish the rendezvous task, but also has a higher control accuracy.

REFERENCES

[1] X. J. Song and S. F. Lu, "Attitude maneuver control of liquid-filled spacecraft with unknown inertia and disturbances," *J. Vib. Control*, vol. 25, no. 8, pp. 1460–1469, Apr. 2019.
[2] Q. Zhao and G. Duan, "Adaptive finite-time tracking control of 6DOF spacecraft motion with inertia parameter identification," *IET Control Theory Appl.*, vol. 13, no. 13, pp. 2075–2085, Sep. 2019.
[3] Z. Zhu and Y. Guo, "Adaptive coordinated attitude control for spacecraft formation with saturating actuators and unknown inertia," *J. Franklin Inst.*, vol. 356, no. 2, pp. 1021–1037, Jan. 2019.
[4] Z. Zhu and Y. Guo, "Adaptive fault-tolerant attitude tracking control for spacecraft formation with unknown inertia," *Int. J. Adapt. Control Signal Process.*, vol. 32, no. 1, pp. 13–26, Jan. 2018.
[5] Q. Li, J. Yuan, and B. Zhang, "Extended state observer based output control for spacecraft rendezvous and docking with actuator saturation," *ISA Trans.*, vol. 88, pp. 37–49, May 2019.
[6] Q. Li, J. Yuan, B. Zhang, and H. Wang, "Artificial potential field based robust adaptive control for spacecraft rendezvous and docking under motion constraint," *ISA Trans.*, vol. 95, pp. 173–184, Dec. 2019.
[7] L. Sun and W. Huo, "Robust adaptive relative position tracking and attitude synchronization for spacecraft rendezvous," *Aerosp. Sci. Technol.*, vol. 41, pp. 28–35, Feb. 2015.
[8] K. Xia and W. Huo, "Disturbance observer based fault-tolerant control for cooperative spacecraft rendezvous and docking with input saturation," *Nonlinear Dyn.*, vol. 88, no. 4, pp. 2735–2745, Jun. 2017.
[9] S. Sharma, C. Beierle, and S. D'Amico, "Pose estimation for non-cooperative spacecraft rendezvous using convolutional neural networks," in *Proc. IEEE Aerosp. Conf.*, Mar. 2018, pp. 1–12.
[10] K. Zhang and M. A. Demetriou, "Adaptive neural network control of spacecraft rendezvous using nonlinear dynamical models in the presence of J2 perturbations," in *Proc. AIAA Guid., Navigat., Control Conf.*, Jan. 2018, p. 1105.
[11] K. Xia and W. Huo, "Robust adaptive backstepping neural networks control for spacecraft rendezvous and docking with uncertainties," *Nonlinear Dyn.*, vol. 84, no. 3, pp. 1683–1695, May 2016.
[12] L. Sun and W. Huo, "Adaptive fuzzy control of spacecraft proximity operations using hierarchical fuzzy systems," *IEEE/ASME Trans. Mechatronics*, vol. 21, no. 3, pp. 1629–1640, Jun. 2016.
[13] L. Sun and Z. Zheng, "Saturated adaptive hierarchical fuzzy attitude-tracking control of rigid spacecraft with modeling and measurement uncertainties," *IEEE Trans. Ind. Electron.*, vol. 66, no. 5, pp. 3742–3751, May 2019.
[14] A. Kosari, H. Jahanshahi, and S. A. Razavi, "An optimal fuzzy PID control approach for docking maneuver of two spacecraft: Orientational motion," *Eng. Sci. Technol., Int. J.*, vol. 20, no. 1, pp. 293–309, Feb. 2017.
[15] A. Kosari, H. Jahanshahi, and S. A. Razavi, "Optimal FPID control approach for a docking maneuver of two spacecraft: Translational motion," *J. Aerosp. Eng.*, vol. 30, no. 4, Jul. 2017, Art. no. 04017011.
[16] N. Wan, W. Yao, and M. Shi, "A composite robust fault-tolerant control scheme for limited-thrust spacecraft rendezvous in near-circular orbits," *J. Dyn. Syst., Meas., Control*, vol. 139, no. 12, Dec. 2017, Art. no. 121009.
[17] R. Fonod, D. Henry, C. Charbonnel, E. Bornschlegl, D. Losa, and S. Bennani, "Robust FDI for fault-tolerant thrust allocation with application to spacecraft rendezvous," *Control Eng. Pract.*, vol. 42, pp. 12–27, Sep. 2015.
[18] B. Jiang, Q. Hu, and M. I. Friswell, "Fixed-time rendezvous control of spacecraft with a tumbling target under loss of actuator effectiveness," *IEEE Trans. Aerosp. Electron. Syst.*, vol. 52, no. 4, pp. 1576–1586, Aug. 2016.
[19] Q. Hu, W. Chen, and L. Guo, "Fixed-time maneuver control of spacecraft autonomous rendezvous with a free-tumbling target," *IEEE Trans. Aerosp. Electron. Syst.*, vol. 55, no. 2, pp. 562–577, Apr. 2019.
[20] Y. Huang and Y. Jia, "Robust adaptive fixed-time 6 DOF tracking control for spacecraft non-cooperative rendezvous," in *Proc. 36th Chin. Control Conf. (CCC)*, Jul. 2017, pp. 3153–3158.

[21] K. Xia and S.-Y. Park, "Adaptive control for spacecraft rendezvous subject to time-varying inertial parameters and actuator faults," *J. Aerosp. Eng.*, vol. 32, no. 5, Sep. 2019, Art. no. 04019063.
[22] K. Xia and Y. Zou, "Adaptive saturated fault-tolerant control for spacecraft rendezvous with redundancy thrusters," *IEEE Trans. Control Syst. Technol.*, early access, Nov. 22, 2019, doi: 10.1109/TCST.2019.2950399.
[23] L. Sun, "Adaptive fault-tolerant constrained control of cooperative spacecraft rendezvous and docking," *IEEE Trans. Ind. Electron.*, vol. 67, no. 4, pp. 3107–3115, Apr. 2020.
[24] Q. Li, J. Yuan, and C. Sun, "Robust fault-tolerant saturated control for spacecraft proximity operations with actuator saturation and faults," *Adv. Space Res.*, vol. 63, no. 5, pp. 1541–1553, Mar. 2019.
[25] P. Singla, K. Subbarao, and J. L. Junkins, "Adaptive output feedback control for spacecraft rendezvous and docking under measurement uncertainty," *J. Guid., Control, Dyn.*, vol. 29, no. 4, pp. 892–902, Jul. 2006.
[26] X. Huang, Y. Yan, Y. Zhou, and J. Yu, "Output feedback control of lorentz-augmented spacecraft rendezvous," *Aerosp. Sci. Technol.*, vol. 42, pp. 241–248, Apr. 2015.
[27] M. J. Sidi, *Spacecraft Dynamics and Control: A Practical Engineering Approach*. Cambridge, U.K.: Cambridge Univ. Press, 1997.
[28] M. D. Shuster, "A survey of attitude representations," *Navigation*, vol. 8, no. 9, pp. 439–517, 1993.
[29] L. Zhang, B. Huang, Y. Liao, and B. Wang, "Finite-time trajectory tracking control for uncertain underactuated marine surface vessels," *IEEE Access*, vol. 7, pp. 102321–102330, 2019.
[30] H. Chen and N. Sun, "Nonlinear control of underactuated systems subject to both actuated and unactuated state constraints with experimental verification," *IEEE Trans. Ind. Electron.*, vol. 67, no. 9, pp. 7702–7714, Sep. 2020.
[31] B. Huang, A.-J. Li, Y. Guo, and C.-Q. Wang, "Fixed-time attitude tracking control for spacecraft without unwinding," *Acta Astronautica*, vol. 151, pp. 818–827, Oct. 2018.
[32] B. Huang, A.-J. Li, Y. Guo, and C.-Q. Wang, "Rotation matrix based finite-time attitude synchronization control for spacecraft with external disturbances," *ISA Trans.*, vol. 85, pp. 141–150, Feb. 2019.
[33] B. Huang, A.-J. Li, Y. Guo, C.-Q. Wang, and J.-H. Guo, "Finite-time fault-tolerant attitude tracking control for spacecraft without unwinding," *Proc. Inst. Mech. Eng., G, J. Aerosp. Eng.*, vol. 233, no. 6, pp. 2119–2130, May 2019.
[34] Z. Shi, C. Deng, S. Zhang, Y. Xie, H. Cui, and Y. Hao, "Hyperbolic tangent function-based finite-time sliding mode control for spacecraft rendezvous maneuver without chattering," *IEEE Access*, vol. 8, pp. 60838–60849, 2020.

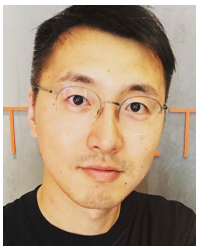

YUAN LIU was born in Beijing, China, in January 1985. He received the bachelor's degree from the Harbin Institute of Technology University, Harbin, China, in 2007, and the master's degree from the Center for Space Science and Applied Research, Chinese Academy of Science, Beijing, China, in 2010. Since 2010, he has been working with the China Academy of Space Technology (CAST). He is currently a Senior Engineer. His current research interests include spacecraft dynamic control and multi-mission planning.

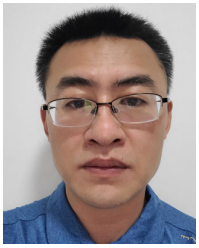

HUI ZHANG received the master's degree from the Nanjing University of Science and Technology, Nanjing, China, in 2013. He is currently a Senior Engineer. His current research interests include spacecraft design plan and project management.

SAI ZHANG received the bachelor's degree in aircraft design and engineering from Harbin Engineering University. His research interests include spacecraft dynamic, fault-tolerant control, and sliding mode control.

HANG LI received the master's degree from the University of Nottingham, U.K., in 2010. He is currently a Senior Engineer. His current research interest includes electronic and communication engineering.

CHENGYI LI received the master's degree from the China Academy of Space Technology, Beijing, China, in 2009. He is currently a Senior Engineer. His current research interest includes spacecraft system design.

JING REN received the bachelor's degree from the Beijing University of Posts and Telecommunications, Beijing, China, in 2013. She is currently an Engineer. Her current research interest includes orbital control method for space rendezvous and docking.

MENGYU QIU received the bachelor's degree from Beihang University, Beijing, China, in 2013. She is currently an Engineer. Her current research interest includes spacecraft on-orbit assembly and preserve.

QI WU received the bachelor's and master's degrees from Northwestern Polytechnical University. He is currently an Engineer. His research interests include spacecraft dynamic and control and sliding mode control.